

**ISSI Innovative Scientific  
Solutions, Incorporated**

2766 Indian Ripple Rd. • Dayton, OH 45440-3638  
937 • 252 • 2706

DEVELOPMENT AND APPLICATION OF AN ADVANCED  
OPTICAL BASED PRESSURE INSTRUMENT FOR  
LOW-SPEED FLOWS

Final Report under Contract F33615-97-C-3005  
Covering the Period  
07 August 1997 - 07 February 1998

19990511 023

# **Development and Application of an Advanced Optical Based Pressure Instrument for Low-Speed Flows**

Final Report under  
Contract F33615-97-C-3005  
Covering the Period  
07 August 1997 – 07 February 1998

Prepared for  
  
Flight Dynamics Directorate  
Air Force Research Laboratory  
Wright-Patterson Air Force Base, OH 45433-7005

7 February 1998

Prepared by  
  
Innovative Scientific Solutions, Inc.  
2786 Indian Ripple Rd.  
Dayton, OH 45440-3638

REPORT DOCUMENTATION PAGE			Form Approved OMB No. 0704-0188	
Public reporting burden for this collection of information is estimated to average 1 hour per response, including the time for reviewing instructions, searching existing data sources, gathering and maintaining the data needed, and completing and reviewing the collection of information. Send comments regarding this burden estimate or any other aspect of this collection of information, including suggestions for reducing this burden, to Washington Headquarters Services, Directorate for Information Operations and Reports, 1215 Jefferson Davis Highway, Suite 1204, Arlington, VA 22202-4302, and to the Office of Management and Budget, Paperwork Reduction Project (0704-0188), Washington, DC 20503.				
1. AGENCY USE ONLY (Leave blank)		2. REPORT DATE 7 Feb 98	3. REPORT TYPE AND DATES COVERED Final 7 Aug 97 - 7 Feb 98	
4. TITLE AND SUBTITLE Development and Application of an Advanced Optical-Based Pressure Instrument for Low-Speed Flows			5. FUNDING NUMBERS C F33615-97-C-3005 G PE PR TA WU	
6. AUTHOR(S) J. D. Jordan L. P. Goss				
7. PERFORMING ORGANIZATION NAME(S) AND ADDRESS(ES) Innovative Scientific Solutions, Inc. 2786 Indian Ripple Road Dayton, OH 45440-3638			8. PERFORMING ORGANIZATION REPORT NUMBER  3005 Final	
9. SPONSORING/MONITORING AGENCY NAME(S) AND ADDRESS(ES) Wright Laboratory, WL/FIMO (Gary A. Dale) Flight Dynamics Directorate Bldg. 24C, Area B 2145 Fifth Street, Ste. 1 Wright-Patterson AFB, OH 45433-7005			10. SPONSORING/MONITORING AGENCY REPORT NUMBER	
11. SUPPLEMENTARY NOTES				
12a. DISTRIBUTION/AVAILABILITY STATEMENT  Approved for public release; distribution unlimited.			12b. DISTRIBUTION CODE	
13. ABSTRACT (Maximum 200 words) The STTR Phase I program targeted the development and application of advanced optical based systems for the determination of surface-pressure distributions on test models in the Subsonic Aerodynamic Research Laboratory (SARL) at Wright Laboratory. The low-speed flows ( $0.1 \leq M \leq 0.5$ ) encountered in the SARL facility effect relatively small changes in surface pressure, typically 1-2 psi about ambient (14.7 psia). As a result, quantitative surface-pressure determination in this environment remained contingent on the development of innovative pressure-sensitive paint (PSP)-coating and optical-measurement technology possessing the requisite sensitivity characteristics. The technical effort encompasses three primary objectives—the development of advanced PSP systems, data-acquisition instrumentation and measurement techniques, and post-processing software. In the Phase I effort, we have coupled the tools of sol-gel-processing technology and inorganic synthetic chemistry for the development of stable PSP's exhibiting tunable performance characteristics. Phase I research has produced sol-gel-based PSP's exhibiting significant improvements in sensitivity about ambient pressure, reduced temperature sensitivity (80%), and fast (>1 kHz) temporal response. Non-intrusive, optical-based measurement techniques capable of accurate pressure measurements in low-speed wind tunnels will find immediate application in commercial- and military-aircraft, automotive, and architectural industries in the United States.				
14. SUBJECT TERMS Pressure-Sensitive Paints, Temperature-Sensitive Paints, Sol-Gels, Pressure Measurements, Temperature Measurements, Low-Speed Flows, Wind Tunnels			15. NUMBER OF PAGES 42	
			16. PRICE CODE	
17. SECURITY CLASSIFICATION OF REPORT UNCLASSIFIED	18. SECURITY CLASSIFICATION OF THIS PAGE UNCLASSIFIED	19. SECURITY CLASSIFICATION OF ABSTRACT UNCLASSIFIED	20. LIMITATION OF ABSTRACT UL	

## Table of Contents

<u>Section</u>		<u>Page</u>
1	INTRODUCTION	1
2	WORK ACCOMPLISHED	1
i.	Development of PSP's for Low-Speed Flow Applications	3
	Base Coat Development	6
	Luminescent-Probe Design	7
	Sol-Gel-Based PSP Optimization	7
	Temperature Sensitivity	10
	Long-Term Stability	10
ii	Development of Improved Data-Acquisition System	11
	Temporal Aspects of Pressure Paints	11
	Step Forcing Function Approaches	13
	Sinusoidal Forcing Function Approaches	13
	Camera Evaluations	16
iii.	Software Development	16
3	POTENTIAL APPLICATIONS	17
	REFERENCES	18
	APPENDIX A	19
	APPENDIX B	32

## List of Figures

<u>Figure</u>	<u>Page</u>
1. PSP/TSP calibration apparatus.	2
2. Typical intensity-decay data for a Ru(dpp) <sub>3</sub> -doped sol-gel-derived PSP.	3
3. Sol-gel-processing chemistry.	4
4. Scanning electron micrographs of sol-gel-derived thin films formed from aerosol deposition (left) and spin coating (right).	5
5. Sol-gel-derived pressure-sensitive-coating architecture.	6
6. Pressure and temperature sensitivity of Pt(TfPP)-based sol-gel and FIB7 PSPs.	7
7. Pressure-sensitivity data for a series of sol-gel-based PSP formulations and FIB7.	8
8. Air jet (1.5 psi) impinging on a ISSI_01 PSP-coated F16 model wing.	9
9. Shelf-life stability of ISSI_01 PSP solution.	10
10. Response of RL circuit to (a) unit and (b) sinusoidal forcing functions.	12
11. Pressure-paint response to sinusoidal modulation, ratio of the integral phases $0 - \pi$ and $\pi - 2\pi$ as a function of the non-dimensional frequency X lifetime product.	14
12. Predicted phase ratio in response to sinusoidal modulation as a function of frequency and pressure-paint lifetime.	15
13. Lifetime of Pt:TfPP in sol-gel binder at room temperature as a function of pressure.	15
14. Predicted phase ratio for Pt:TfPP calibration as a function of pressure and modulation frequency.	16
15. User interface for PSPCALC_3.0 data-processing software.	17

## 1. INTRODUCTION

This final report describes R&D efforts under Air Force Contract F33615-97-C-3005 during the period 7 August 1997 – 7 February 1998. Contributing to the program effort were Dr. Larry Goss, Dr. Jeff Jordan, Dr. William Weaver, Ms. Kelly Navarra, Mr. Darryl Trump, and Mr. Ben Sarka of Innovative Scientific Solutions, Inc. and Professor Daniel Nocera of the Massachusetts Institute of Technology (Academic Partner).

The accurate determination of surface-pressure distributions on aerodynamic test models is critical to the understanding of complex flow phenomena and the validation of computational-fluid-dynamics (CFD) models for simulation of new designs. Conventional surface-pressure measurements are based on the use of pressure taps and transducers. These techniques provide accurate pressure data; however, they are limited to point measurements and limited by the difficulty and expense associated with the installation of an adequate population of pressure taps on the test model.

Pressure-sensitive paint (PSP) technology has emerged as a viable alternative for full-field surface-pressure measurements. In these schemes luminescent molecules are dispersed within a polymeric binder, or paint, which is then applied to the test model of interest. Illumination of the PSP coating with the appropriate excitation frequency induces lower energy light emission from the PSP, with amplitude inversely proportional to the partial pressure of oxygen ( $P_{O_2}$ ). Because oxygen is a fixed-fraction of air, PSP-based systems provide a means of non-intrusive, full-field surface-pressure measurements at relatively low cost very early in the design cycle. In fact, PSP measurements have been used with much success in a variety of low-pressure aerodynamic-test applications. Existing PSP-based measurement systems, however, are not adequately sensitive for use at subsonic speeds, which encompass much of the flight envelope of highly maneuverable air vehicles.

The purpose of this STTR Program is the development of optical-based systems capable of the accurate determination of surface-pressure distributions on test models for low-speed flow applications. Toward this end, the Phase I research effort encompassed three primary objectives including:

- 1) the development of advanced PSPs exhibiting significant improvements in sensitivity and signal output at ambient pressure (14.7 psia) and reduced temperature sensitivity,
- 2) evaluation and identification of stable illumination sources and CCD camera systems characterized by low-noise operation, and
- 3) the investigation of alternative PSP-measurement techniques that do not require the acquisition of a wind-off image.

## 2. WORK ACCOMPLISHED

In the Phase I program, the feasibility of sol-gel-based coatings for the formation of stable PSP platforms exhibiting *tunable* pressure sensitivity was demonstrated. These coatings are

characterized by significant improvements in pressure sensitivity near ambient ( $\sim 6\%/psi$  for  $P > 14.7$  psia), reduced temperature sensitivity ( $< 1\%/^{\circ}C$ ), and very low surface roughness ( $\sim 10^{-6}$  in). In parallel with these efforts, a series of illumination and CCD detection sources were evaluated and leading candidates identified. In addition, alternative measurement techniques were investigated for the acquisition of surface-pressure data, and data-acquisition and post-processing software was developed.

### *Calibration Instrument for Paint Characterization*

In order to characterize our pressure-sensitive coatings, we designed and constructed the apparatus for ground-based testing shown in Fig. 1.

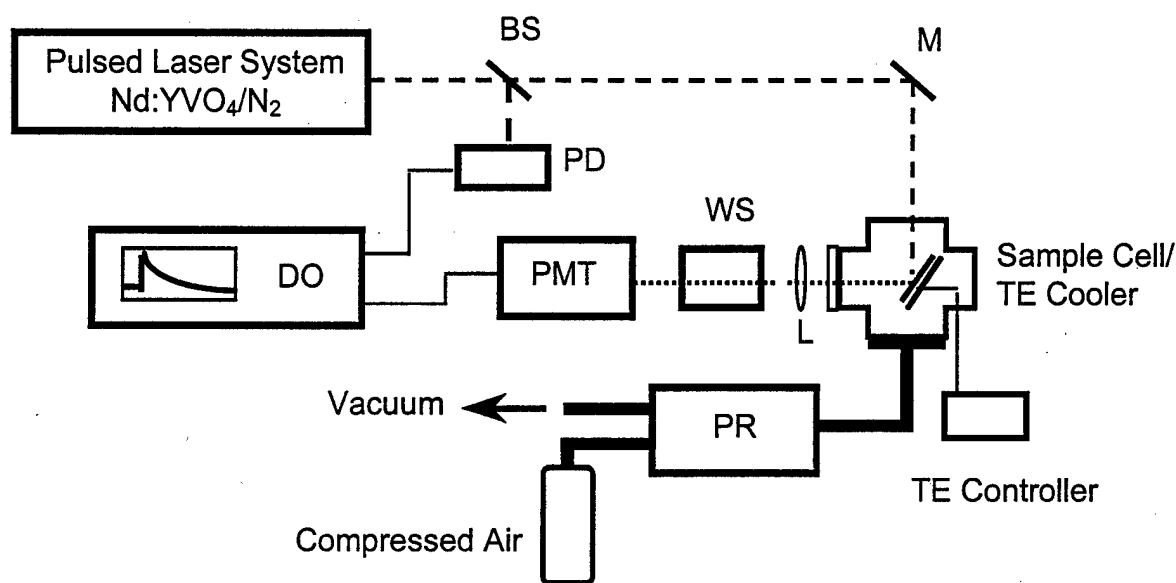


**Figure 1. PSP/TSP calibration apparatus.**

Figure 1 is a schematic of the primary apparatus used to characterize our pressure-sensitive coatings. A fraction of the pulsed output from a N<sub>2</sub> laser (Laser Science, Inc., Model VSL-337) is directed to a photodiode (PD) which triggers a 200-MHz (1-G sample/s) digital oscilloscope (DO, Tektronix, Model TDS 350). The remainder of the beam is directed by a mirror (M) into a four-way cross (Kurt J. Lesker Co., Model QF40-150-X) in which the sample is fixed at a 25° angle with respect to the incident beam. The fluorescence from the coating is collected by a lens (L) and is directed through an optical filter (WS) to isolate the fluorescence from the scattered light. The filtered emission is then directed to the face of a fast-wired photomultiplier-tube (PMT) detector whose output is connected to the oscilloscope. The atmosphere within the four-way cross is controlled by a pressure-regulation device (PR, Druck, Model DPI500) which employs vacuum and compressed air to maintain the cell pressure between 0.05 and 2 atm.

Sample substrates are mounted within the four-way cross on a thermoelectric (TE) cooler for temperature control. The entire system is under automated computer control.

In operation, the cell pressure is incremented, and time-resolved intensity decay traces are collected at each pressure. From these data the excited-state fluorescence lifetimes are recovered, the total intensity determined, and calibration curves produced. Typical data are shown in Figure 2.

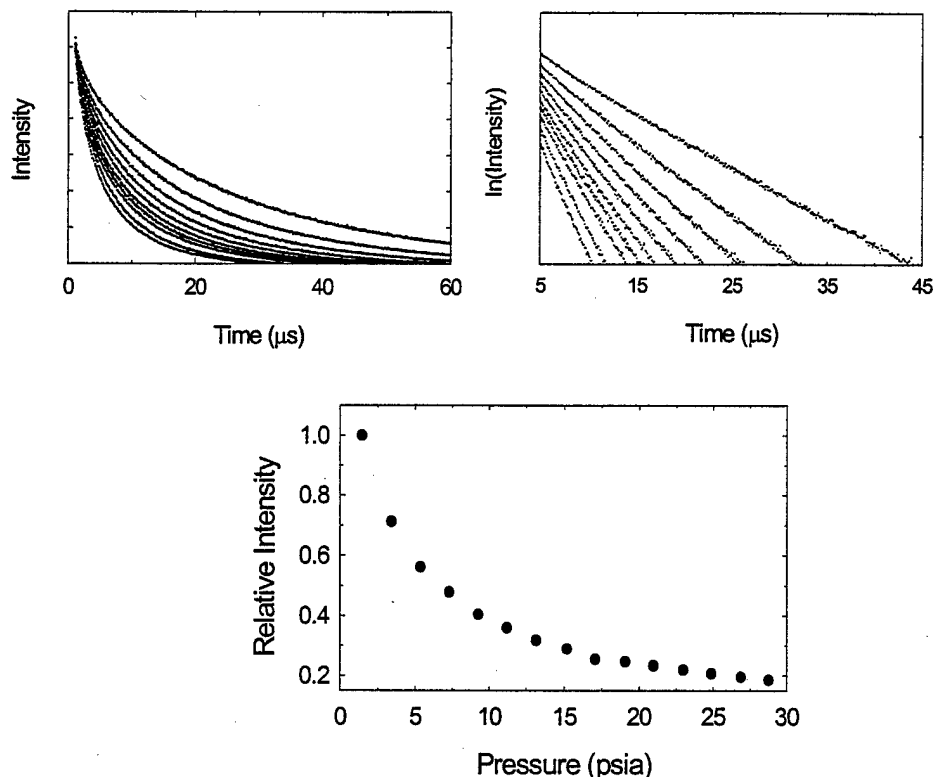


**Figure 2. Typical intensity-decay data for a Ru(dpp)<sub>3</sub>-doped sol-gel-derived PSP.**

Figure 2A shows intensity-vs.-time decay profiles for increasing air pressure. The ln(Intensity) data (Fig. 2B) indicate that the intensity-decay kinetics are well characterized by a single-exponential decay model, facilitating lifetime-based imaging analysis. Finally, the relative intensities and lifetimes are recovered from the intensity-decay traces [ $I(t) = \exp(-t/\tau_i)$ ] and plotted as a function of pressure to obtain the sample calibration (Fig. 2C).

#### **i. Development of PSP's for Low-Speed-Flow Applications**

The application of PSP technology to low-speed-flow applications is contingent on significant improvements in sensitivity at near-ambient pressure ( $14.7 \pm 2$  psia). The salient criteria

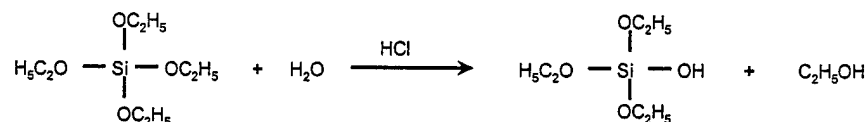


governing pressure sensitivity include probe luminescence lifetime ( $\tau$ ), quantum efficiency ( $\phi_e$ ), and accessibility to molecular oxygen ( $O_2$ ). Lifetime and quantum-efficiency characteristics of a PSP are dominated by the photophysics of the luminescent species. Probe accessibility to  $O_2$  determines the efficiency of the quenching process and is modulated by the porosity or void volume of the polymeric support matrix.

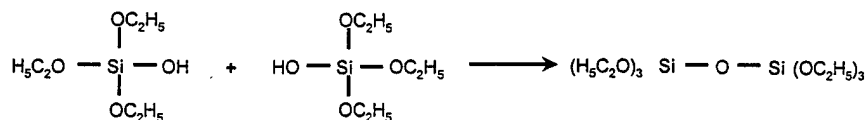
For these reasons, we have developed a two-fold approach to PSP optimization. Luminescent species exhibiting appropriate lifetime (1 - 100  $\mu$ s), quantum-efficiency ( $> 0.5$ ), and stability characteristics are being engineered by the research group of Professor Daniel G. Nocera at the Massachusetts Institute of Technology. Probe species were received by ISSI personnel and incorporated into the advanced PSP architectures under development.

In the design of PSP coatings, the polymeric support dictates the thermal and mechanical stability, adherence characteristics, and surface roughness, while contributing to the pressure and temperature sensitivity and temporal response. Controlling these parameters would allow the formation of PSP systems ideally suited for particular test conditions (P, T) of interest. Recently, the development of PSP's has been complemented by sol-gel technology. The sol-gel-process allows the formation of controlled-pore glasses under ambient temperature and pressure conditions. Sol-gel processing involves the transition of a solution phase into a gel; this is followed by densification and loss of solvent, ultimately resulting in a solid, optically transparent glass. The sol-gel chemistry is represented by the following five-step process:

*Hydrolysis* TEOS, tetraethylorthosilicate



*Condensation*



*Polycondensation*

Formation of 3D matrix

*Aging/Drying*

Expulsion of solvent  
Composite strength increased

**Figure 3. Sol-gel-processing chemistry.**

The process is initiated by the acid or base-catalyzed hydrolysis of a metal or semi-metal alkoxide such as tetraethylorthosilicate (TEOS) to form the hydrated product. Condensation of these moieties results in the formation of metal-oxygen-metal bonds (Si-O-Si) and a colloidal mixture termed a sol. Polycondensation of these species results in the formation of a three-

dimensional network and macroscopic solid as defined by the gelation point. Subsequent aging and drying of the composite film results in the expulsion of solvent from the matrix, which increases the composite strength. Host composites for chemical-sensing applications can be easily produced in this manner by incorporating recognition elements (RE, e.g., probe molecules) directly into the sol-gel-precursor solution, followed by thin-film deposition. In this manner, the RE is entrapped within the porous matrix, and a significant population remains accessible to the external analyte. In addition, the molar ratio of sol-gel precursors, hydrolysis time and temperature, and aging and drying conditions affect the sol-gel-processing chemistry and, thus, the physicochemical properties of the final composite (e.g., porosity, polarity). In general, our experiments have indicated that the optimum-quality films are produced using TEOS:ethanol:water:HCl:KOH molar ratios of  $1:2:2:10^{-3}:10^{-3}$ , in concert with six total hours of hydrolysis at 22°C prior to PSP formation.

Conventional methods of sol-gel thin-film formation include dip-coating and spin-coating techniques in which a test substrate is submerged within a sol-gel solution, or mechanically rotated to coat a surface via centrifugal force. Both methods require large volumes of coating solution (paint), the majority of which is wasted in the coating process. Moreover, neither technique is amenable to uniform thin-film formation on test articles of irregular geometries such as aerodynamic test models. Therefore, it was clear that new methods for the formation of thin, uniform films were required if the advantages of sol-gel-processed materials for PSP development were to be fully exploited. To this end, we developed both ultrasonic- and pressure-based aerosol deposition techniques for the formation of thin, uniform sol-gel-derived PSP's. Previous work has shown that the deposition approach used can dramatically affect sensor performance in addition to macroscopic material properties. For example, scanning electron microscopy (SEM) and surface-profile experiments were performed for both aerosol-generated and spin-coated sol-gel-processed films, and the results are shown in Figure 4.

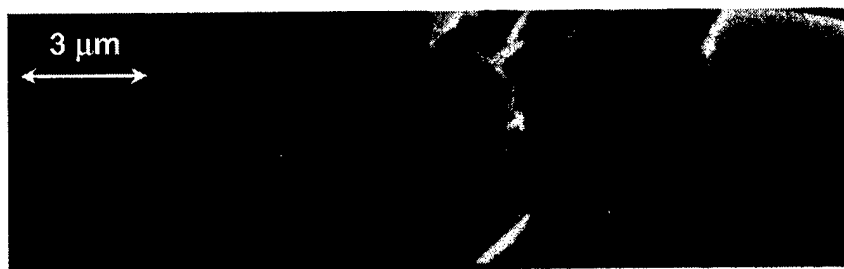


**Figure 4. Scanning electron micrographs of sol-gel-derived thin films formed from aerosol deposition (left) and spin coating (right).**

Both films shown above were 2.0 μm in thickness. It is clear that the aerosol-deposition approach produced a thin, uniform surface with very low surface roughness (~50 nm). In contrast, the conventional spin-coating technique produced an unstable, highly-cracked film that was unsuitable for PSP applications.

The use of sol-gel-derived composite coatings as platforms for chemical and biological sensors has been demonstrated. Typically, successful applications of these coatings involve deposition onto silicon substrates such as glass or quartz. Adaptation of this technology for commercial and military wind-tunnel applications employing test models made from various metallic and ceramic materials introduces two additional challenges associated with coating adherence and substrate-induced quenching of the entrapped probe species via phonon coupling to the surface. To overcome these difficulties, we developed the coating architecture illustrated in Figure 5.



**Figure 5. Sol-gel-derived pressure-sensitive-coating architecture.**

In this approach, a bare-aluminum test substrate is cleaned and coated with a white base-coat layer. The base coat serves simultaneously to improve sol-gel adherence to the surface, eliminate substrate-induced quenching of the sol-gel-entrapped probe, maintain pressure sensitivity, and mask test-surface irregularities.

Sol-gel-based coatings serve as the primary binder matrix, primarily as a result of their ease of preparation, application, and removal from the test model, compatibility with probe solvents, smooth surface finish, and long-term stability. In addition, control over the sol-gel-processing chemistry provides a means of tailoring the physical properties of the silicon-based coatings and, thus, the performance characteristics of the resulting PSP. Phase I research produced aerosol-based deposition approaches for the formation of thin ( $< 5\text{-}\mu\text{m}$ ) sol-gel-based PSPs. As a result, a robust PSP platform has been developed that is suitable for the incorporation of luminescent species engineered for specific pressure and temperature regimes of interest.

#### *Base-Coat Development*

In the sol-gel-based PSP platform, the base coat generally serves to stabilize the probe-doped sol-gel-derived active layer, activate the entrapped probe, improve adherence characteristics, and provide a screen layer suitable for uniform PSP deposition. Phase I research demonstrated that stable base-coat films could be achieved through the use of commercially available white spray paints. However, these base coats can impart greater thermal sensitivity to the PSP, resulting in pressure-measurement uncertainties due to temperature-dependent intensity variations. In fact, Phase I research has shown that temperature sensitivity can vary by as much as a factor of three for the same PSP deposited onto a variety of commercially available base-coat layers.

## Luminescent-Probe Design

For low-speed flow applications, the ideal luminescent complex would be characterized by high quantum yield (luminescence efficiency), a lifetime in the 1-10  $\mu$ s range, and low temperature sensitivity. Many inorganic luminescent complexes are efficient emitters with lifetimes in this range. Moreover, inorganic complexes are characterized by low-energy vibrations that are typically populated at room temperature. Thus, if an inorganic complex is a bright emitter at room temperature, its luminescence will be maintained as the temperature is increased without a population of new thermally activated nonradiative-decay pathways. The result is a PSP exhibiting minimized sensitivity to temperature. Finally, probe functionality groups can be synthetically engineered to control and improve solubility in alcohol-based sol-gel-processed precursor solutions.

Luminescent species produced in Professor Nocera's laboratory include a platinum dimer and a series of ruthenium compounds. PSPs were produced by incorporating these species within sol-gel and silicone coatings. Calibration results demonstrate that these PSPs exhibit lifetimes on the order of 500 ns and negligible or low sensitivity to pressure. The relatively short lifetime indicates that fluorescence emission (singlet-to-singlet transition) dominates the desired, longer-lived ( $\geq 1$   $\mu$ s) phosphorescence (triplet-to-singlet transition). Ongoing efforts of the Nocera Group focus on synthetically engineering probes exhibiting room-temperature phosphorescence while maintaining insensitivity to temperature (Appendix B).

## Sol-Gel-Based PSP Optimization

To date, the highest ambient-pressure sensitivity has been exhibited by platinum meso-Tetra (pentafluorophenyl) porphine (Pt(TfPP))-doped sol-gel-based PSPs. The PSP platform is composed of a sol-gel-based PSP overlaying a white-paint base coat. The final material exhibits mechanical stability over a broad temperature range, very low surface roughness, and ease of application and removal from the model surface. In Phase I research, a series of Pt(TfPP)/sol-gel-based PSP formulations has been produced and characterized in terms of pressure (1 - 30 psia) and temperature (15 - 35°C) sensitivity. Figure 6 shows typical pressure-sensitivity data plotted as a function of temperature for a Pt(TfPP)-based sol-gel (ISSI\_01) and a proprietary formulation from the research group of Professor Martin Gouterman at the University of Washington (FIB7).

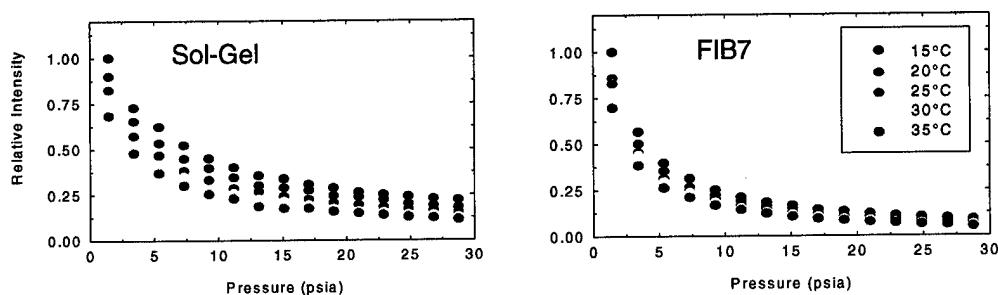


**Figure 6. Pressure and temperature sensitivity of Pt(TfPP)-based sol-gel and FIB7 PSPs.**

The results indicate that the FIB7 PSP exhibits less temperature sensitivity ( $\sim 0.2\%/^{\circ}\text{C}$ ) than ISSI\_01 ( $\sim 0.5\%/^{\circ}\text{C}$ ) at ambient pressure and comparable sensitivity ( $\sim 0.8\%/^{\circ}\text{C}$ ) at low pressure ( $\sim 1$  psia). The pressure sensitivity of the ISSI\_01 PSP, however, is slightly greater than that of FIB7 for small changes in pressure above ambient. Moreover, the ISSI sol-gel-based PSP at 14.7 psia maintains  $\sim 25\%$  of the total intensity (relative to 1 psia), while the FIB7 PSP exhibits less than one-half of this signal level ( $\sim 10\%$ ). This indicates that for PSPs exhibiting comparable signal, the superior S/N ratio observed at ambient pressure for the sol-gel-based PSP will result in greater pressure resolution for low-speed-flow applications.

Figure 7 shows pressure-sensitivity data for a series of Pt(TfPP)-based PSPs produced by the conventional approach (TfPP solution deposited onto a white-paint-coated substrate) and entrapped within sol-gel-derived thin films (ISSI) and for a proprietary polymer formulation (FIB7).

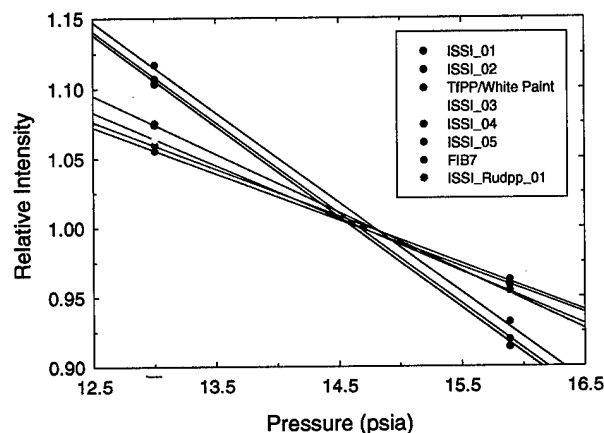


**Figure 7. Pressure-sensitivity data for a series of sol-gel-based PSP formulations and FIB7.**

These data illustrate the utility of sol-gel processing as a means of tailoring PSP performance characteristics. For example, subtle perturbations to the sol-gel-processing chemistry increased the near-ambient pressure sensitivity by a factor of two. Moreover, the ISSI Pt(TfPP)/sol-gel-based PSP formulations are competitive with the proprietary FIB7 PSP of the University of Washington, developed by McDonnell Douglas and currently employed by NASA Ames Research Center and Arnold Engineering Development Center for wind-tunnel testing. Phase II research will provide a mechanism for the advanced development of sol-gel-based PSPs to further enhance the sensitivity at near-ambient pressure conditions. The resulting PSPs will be state-of-the-art pressure-sensitive coatings for low-speed wind tunnel testing and gain a strong market share in PSP commercialization.

Quantitative surface-pressure measurements on scale models within the SARL facility introduce additional challenges associated with illumination and coating nonuniformities and CCD-camera anomalies. To demonstrate the enhancement in pressure sensitivity on an aerodynamic surface, an F16 model ( $\sim 1/100$  scale) was coated with ISSI\_01 PSP, and images were acquired under the influence of a 1.5-psi air jet impinging on the model wing. For these experiments excitation was

provided by the CW output from a Nd:YVO<sub>4</sub> laser operating at 532 nm, and single-shot images were acquired with a scientific-grade 16-bit back-lit CCD camera (Pixelvision) using a 1-s integration. The “wind-on” image acquired at condition was ratioed with the “wind-off” reference image to produce the pressure map shown in Figure 8.

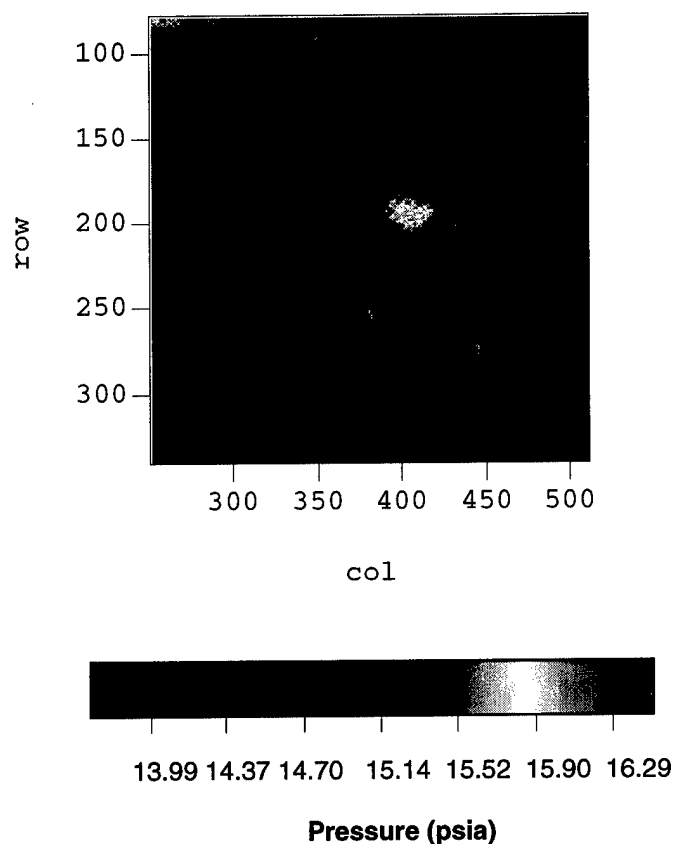


**Figure 8. Air jet (1.5 psi) impinging on a ISSI\_01 PSP-coated F16 model wing.**

The point of jet impingement (red-yellow region) is clearly visible in the ratioed image against the ambient (14.7 psia) background. These data illustrate the utility of the sol-gel-based platform for quantitative visualization of surface-pressure fields in low-speed-flow applications. Previous work has shown that the sol-gel-based PSPs exhibit high- (423 K) and low-temperature (77 K) stability, very low surface roughness ( $\sim 2\text{e-}6$  in), negligible temperature-dependent viscosity changes (reduced temperature sensitivity), and tunable pressure sensitivity. In addition, the chemical nature of the sol-gel solution allows the incorporation of probe species from a wide variety of solvents, greatly minimizing solubility problems. As a result, the sol-gel platform is well suited for the incorporation of inorganic luminescent probes synthesized by the Nocera

Group and the development of advanced PSP coatings for a wide variety of military and commercial low-speed-flow applications.

### *Temperature Sensitivity*

PSP temperature sensitivity is governed by the non-radiative decay pathways inherent in the probe molecule and a series of binder effects including probe activation. In Phase II research, a three-fold approach will be pursued for minimizing PSP thermal stability: 1) incorporating luminescent species synthetically engineered by the Nocera Group for low-temperature sensitivity, 2) tailoring the sol-gel chemistry and post-processing conditions to minimize temperature-dependent viscosity effects, and 3) identifying probe-activation agents suitable for the development of an optimized base coat. This strategy is supported by Phase I results which showed that: 1) PSPs based on the ruthenium probes synthesized by the Nocera Group exhibit negligible sensitivity to temperature, 2) sol-gel-processing time can affect the thermal stability of the resulting PSP, and 2) the temperature sensitivity for ISSI\_01-based PSPs deposited onto an array of commercially available white base coats varied by as much as a factor of three.

### *Long-Term Stability*

Phase III marketing of advanced PSPs optimized for use in low-speed wind tunnels will require that the PSP solutions remain stable under ambient storage. The stability of the sol-gel-based PSP formulations was determined by preparing a bulk solution of Pt(TfPP)-doped sol gel and storing it in the dark at room temperature. Aliquots were removed periodically and PSPs produced and calibrated. The resulting pressure-sensitivity data are shown in Figure 9.

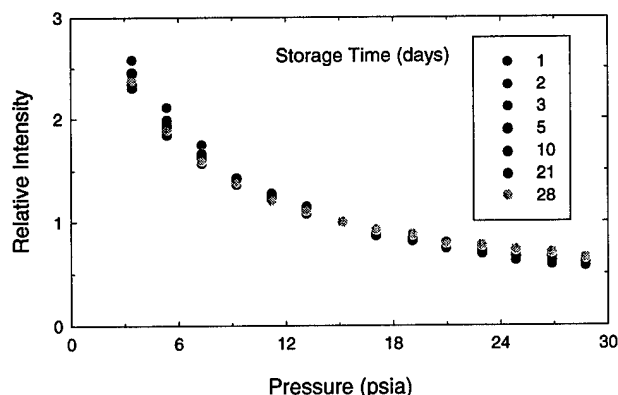


**Figure 9. Shelf-life stability of ISSI\_01 PSP solution.**

Phase I research indicates that the ISSI\_01 PSP is stable when stored in the dark over a period of at least one month, minimizing error in PSP preparation, calibration, and storage and facilitating transfer to military and commercial entities for use in wind-tunnel facilities in Phase III commercialization efforts.

## ii. Development of Improved Data-Acquisition System

The routine use of PSP technology has been plagued with difficulties associated with non-uniformity in the paint and illumination field, self-illumination, and paint photodegradation. In the conventional approach, errors associated with these effects are minimized by relating pressure to the ratio of a "wind-on" image acquired at condition to a "wind-off" reference image. This process becomes problematic because of difficulties associated with the complex-coordinate mapping of the reference image to the spatially distorted run image. Alternative measurement approaches that do not require the wind-off image were investigated in the Phase I research. Specifically, in collaboration with Professor John Sullivan of Purdue University, we performed a laboratory-based comparison of 1D-scanning (Purdue) and 2D-imaging (ISSI) approaches for the acquisition of PSP data. Initial experiments were performed at ISSI facilities in December of 1997. A report authored by Professor Sullivan highlights the accomplishments of this effort and is included as Appendix A to this final report. In addition to the 1D lifetime method of professor Sullivan, 2D lifetime imaging methods were investigated and are discussed below.

*Temporal Aspects of Pressure Paints.* A close analogy to the temporal behavior of pressure paint is that of a simple resistor-inductance (RL) circuit. The response of this circuit to a time-variant change in voltage is given by

$$Ri + L \frac{di}{dt} = Vu(t) \quad (1)$$

where R is the resistance of the circuit, L the inductance, i the current, and Vu(t) the time-variant voltage. The response of the circuit to a unit forcing function is given by

$$i = \left( \frac{V}{R} - \frac{V}{R} e^{-\frac{Rt}{L}} \right) u(t) \quad (2)$$

where V/R represents the steady-state or forced response of the circuit and the exponential term represents the natural response. The forced and natural responses of the circuit to a unit forcing function are graphically depicted in Fig. 10a. Replacing the ratio R/L with 1/τ, the ratio V/R with I<sub>o</sub>, and the current with I, the response of pressure paint to a unit excitation function can be described by

$$I = (I_o - I_o e^{-t/\tau}) u(t) \quad (3)$$

From Eq. (3) and Fig. 10a, it can be seen that the pressure-paint responds to a step turn-on of the excitation light by exponentially increasing until the steady state value of I<sub>o</sub> is reached. The paint responds to the turn-off of the light by an exponential decrease in its emission. To determine the lifetime, τ, of the paint (and, therefore, the pressure), one can measure either the turn-on or the turn-off response to a unit forcing function. This approach will be discussed in detail below.



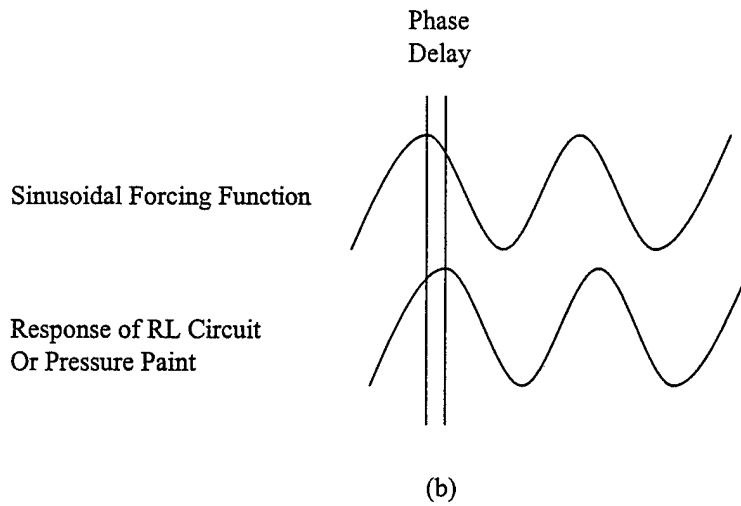
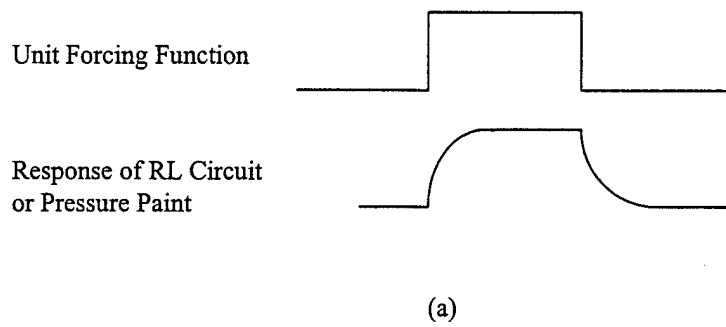


**Figure 10. Response of RL circuit to (a) unit and (b) sinusoidal forcing functions.**

Another interesting feature of the RL circuit is its response to a sinusoidal forcing function. In this case Eq. (1) becomes

$$L \frac{di}{dt} + Ri = V_m [1 + \sin(\omega t)] \quad (4)$$

where  $\omega = 2\pi f$  and  $f$  is the modulation frequency. The solution to the response of the sinusoidal forced function is given by

$$i(t) = V_m \left[ 1 + \frac{1}{\sqrt{R^2 + \omega^2 L^2}} \sin(\omega t - \tan^{-1} \frac{\omega L}{R}) \right] \quad (5)$$

Equation (5) predicts the circuit responses to the sinusoidal function by attenuation of  $V_m$  by the square-root portion of Eq. (5) and by introduction of a phase lag given by the  $\tan^{-1}$  portion of Eq. (5). Making the substitutions mentioned earlier for pressure paints, the paint response to a

sinusoidal forcing function can be predicted and is given by

$$I(t) = I_o \left[ 1 + \frac{1}{\sqrt{1 + \omega^2 \tau^2}} \sin(\omega t - \phi) \right] \quad \text{where} \quad \tan \phi = \omega \tau \quad (6)$$

As with the RL circuit, the paint response to a sinusoidal forcing function is characterized by an attenuation of the intensity and a phase lag which are pictorially depicted in Fig. 10b. It should be possible to measure the attenuation and phase lag to determine the lifetime,  $\tau$ , and, thus, measure the pressure of the painted surface. The different approaches to measuring the paint lifetime by its response to either a step or a sinusoidal forcing function are discussed in detail below.

*Step-Forcing-Function Approaches.* In the step-function approach, a laser source is normally used for excitation; however, a short lamp pulse can also be used for long-lifetime paints. The emission decay can be captured with two-gated camera systems,<sup>1</sup> a fast sampling camera,<sup>2</sup> or a cross-correlation camera.<sup>3</sup> The net result is a two-dimensional measurement of the lifetime of a painted surface. Because of the high noise of gated intensified cameras, fast-sampling or cross-correlation cameras are better choices for lifetime measurements. In the fast-sampling camera technique, a high-speed camera (1 million frames/second) is used to capture the paint emission as a function of time. The images are then ratioed to determine the lifetime of the painted surface. The potential problem with this approach is the limited signal-to-noise ratio likely to be encountered with single-shot operation. Averaging multiple shots will significantly improve this situation, making this a viable approach. An alternative approach to step-function measurements involves the use of a cross-correlation camera. This camera is unique because it allows two images with time separations greater than 300 ns to be captured and compared for analysis purposes. In this case, the first image is taken of the painted surface during steady-state light excitation; immediately following this the light is turned off, and the second image records the decay curve of the emission. The ratio of the two images is a unique function of the lifetime and would allow two-dimensional pressure measurements to be made. The advantages of the step-function lifetime approaches include 1) elimination or reduction of the need for a wind-off measurement, 2) elimination or reduction in the sensitivity of the technique to lighting non-uniformity, and 3) elimination or reduction in the sensitivity of the technique to paint non-uniformity. The drawback of the direct lifetime approach is the requirement for novel expensive cameras.

*Sinusoidal-Forcing-Function Approaches.* The sinusoidal approach to measuring lifetime by phase involves sine-wave or square-wave modulation of the excitation light and observation of the attenuation or phase lag of the paint emission response with a phase-sensitive detector. A variation of this method is used in the point-wise scanning systems employed for pressure measurements<sup>4-5</sup> where the excitation laser is modulated with a sine-wave and the phase delay of the resulting emission signal is measured with a lock-in. The phase-angle is a sensitive function of the lifetime and excitation frequency. A camera adaptation for phase measurements is possible and will be explored in the Phase II program.<sup>6</sup> In this approach, the paint sample is excited with sinusoidal illumination and recorded with a phase-sensitive camera. A standard CCD camera is made phase sensitive by incorporation of a high-speed shutter which allows the 0

-  $\pi$  phase of the signal to be recorded on the first camera exposure and the  $\pi - 2\pi$  phase of the signal to be recorded on the second exposure.<sup>6</sup> Ratioing the images results in a function that is sensitive to paint-emission lifetime and excitation frequency, as shown in Fig. 11. The x-axis of the graph in Fig. 11 is a non-dimensional number that represents the product of the excitation frequency and the emission lifetime. The curve in this figure was calculated by ratioing the phase integrals ( $0 - \pi$  by  $\pi - 2\pi$ ) of Eq. (6). The phase-ratio method is most sensitive for a non-dimensional frequency-lifetime product less than 0.5. Figure 12 displays the phase ratio for various paint lifetimes as a function of excitation frequency. Careful selection of the excitation frequency can enhance the sensitivity of lifetime measurements and, thus, the surface pressure. The sensitivity of the approach is best demonstrated by incorporation of the lifetimes of a real pressure paint. Figure 13 shows the measured lifetime of the probe molecule Pt:TfPP in a sol-gel binder as a function of pressure at room temperature. These data can be substituted into the curve shown in Fig. 12 to yield the phase ratio as a function of excitation frequency. The results of this operation are shown in Fig. 14 and indicate a strong dependence on both the lifetime and the excitation frequency. A sensitivity analysis of the data, shown in Fig. 14, indicates that for pressures around 1 atm (14.7 psi), a modulation frequency between 10 and 15 kHz is ideal.

The major advantage of phase-measurement techniques is the ability to tune the pressure sensitivity by varying the modulation frequency. For example, the sensitivity of the technique can be enhanced at low pressures using low modulation frequencies and at high pressures using high modulation frequencies. This ability to tune the sensitivity offers a high degree of flexibility to the user when planning experiments in different pressure regimes.

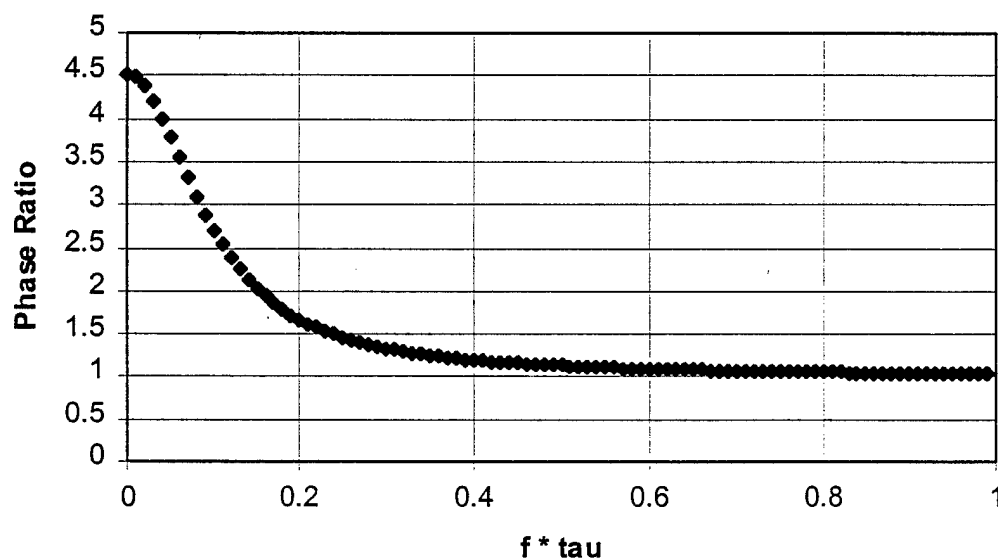


**Figure 11. Pressure-paint response to sinusoidal modulation; ratio of the integral phases  $0 - \pi$  and  $\pi - 2\pi$  as a function of the non-dimensional frequency X lifetime product.**

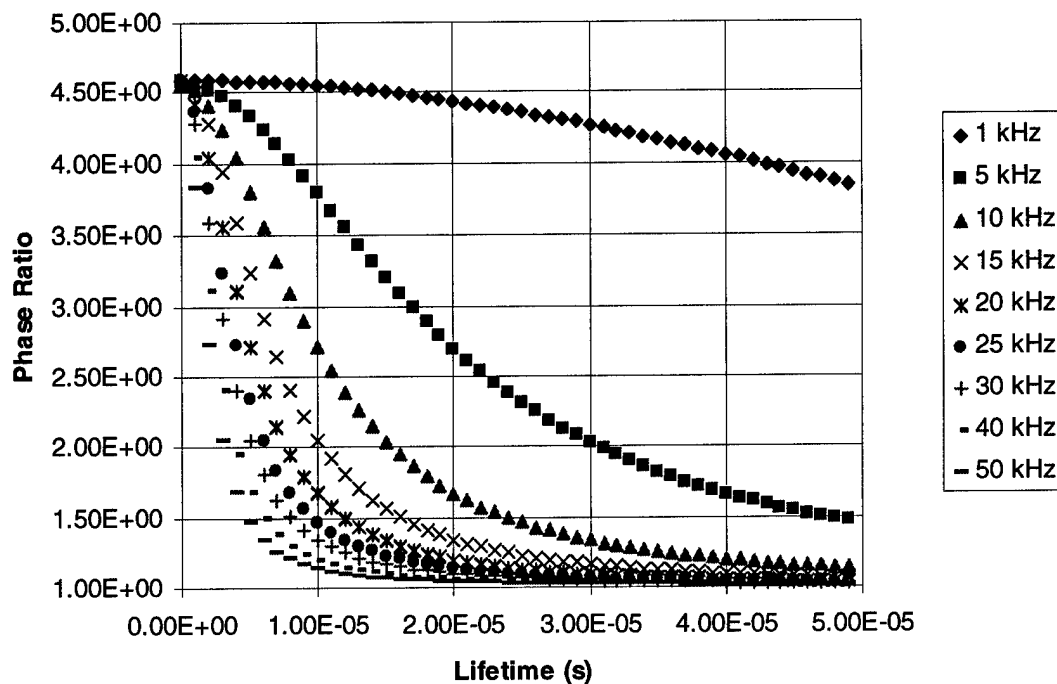


Figure 12. Predicted phase ratio in response to sinusoidal modulation as a function of frequency and pressure-paint lifetime.

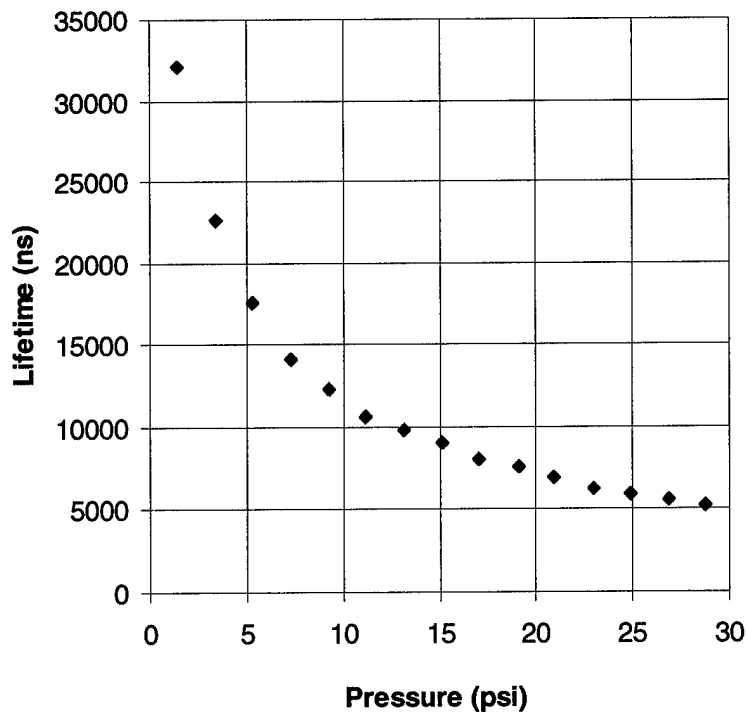
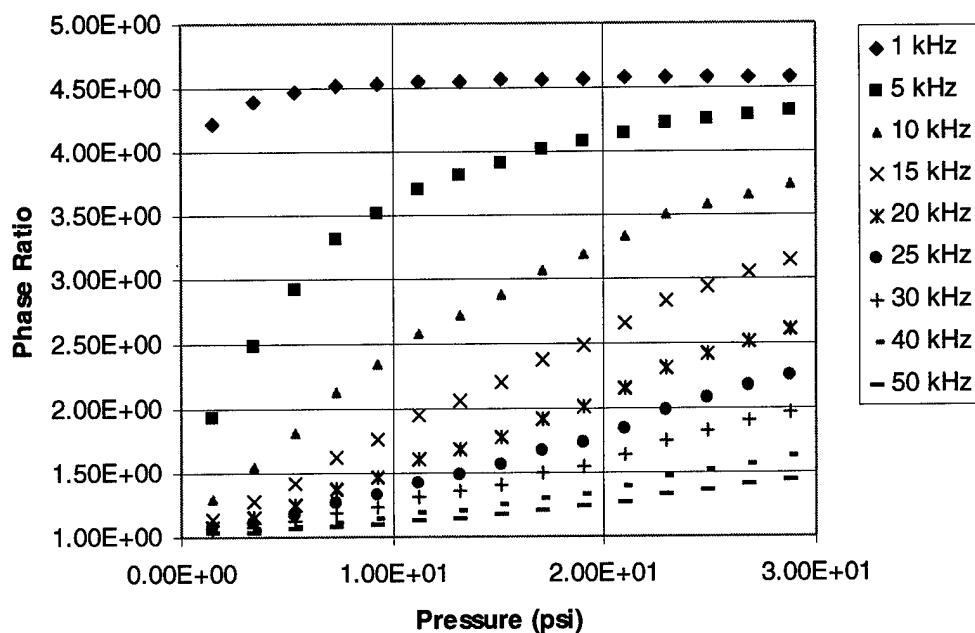


Figure 13. Lifetime of Pt:TfPP in sol-gel binder at room temperature as a function of pressure.



**Figure 14. Predicted phase ratio for Pt:TfPP calibration as a function of pressure and modulation frequency.**

*Camera Evaluations.* A comparative evaluation of intensified (Princeton Instruments) and back-lit CCD cameras (Photometrics, Pixelvision) was performed to identify detection systems exhibiting low-noise characteristics and large dynamic range. These experiments demonstrated the improved S/N ratios possible with the back-lit CCD cameras, with the intensified CCD exhibiting ten-fold greater noise. Based on these data, back-lit CCD cameras are recommended for the development of the PSP data-acquisition system in the Phase II Program.

### iii. Software Development

In support of Phase I PSP development, software was written in a LabWindows CVI format for full automation of the data acquisition and reduction associated with the PSP calibration apparatus (Figure 1). The user interface for PSPCALC 3.0 data-analysis software following calibration of a Pt(TfPP)/sol-gel-based PSP is shown in Figure 15.

In this scheme, master files associated with pressure-calibration data are selected for the range of temperatures investigated. Individual intensity-decay traces are fit to a single-exponential decay function within a user-defined intensity range. From these data, lifetime and intensity vs. pressure calibration curves are generated and the associated Stern-Volmer plots produced. Following this analysis, the results can be displayed in any form desired by the user and written

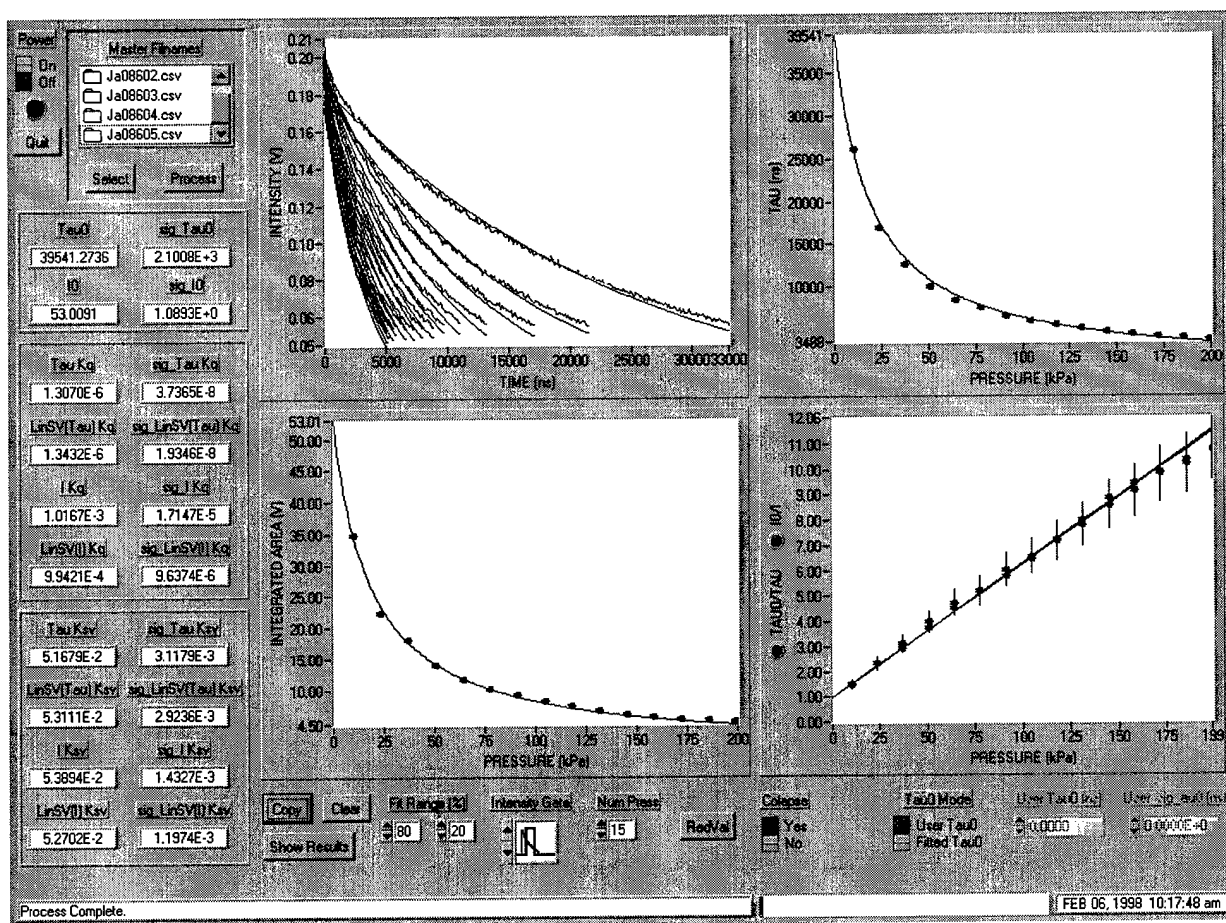


**Figure 15. User interface for PSPCALC\_3.0 data-processing software.**

to an Excel file for storage. The fully automated software package greatly facilitates analysis of PSP data, allowing rapid screening of candidate PSP composite materials.

In the Phase II research, data-acquisition software will be written to provide simultaneous control over the illumination and detection sources and subsequent data storage, with the final goal of integrating these modules into the Greenboot Program. In preparation for this eventuality, ISSI and AFRL/VA personnel received Greenboot training from Boeing personnel at Arnold Engineering Development Center (AEDC).

### 3. POTENTIAL APPLICATIONS OF THE EFFORT

Non-intrusive, optical-based techniques capable of accurate pressure measurements in low-speed wind tunnels would find immediate application in commercial- and military-aircraft, automotive, and architectural industries in the United States. The advanced diagnostic systems developed under this STTR program will have a significant impact on the advancement of ground testing of complex aerodynamic flow systems, including ongoing and recently initiated ventures such as the Air Force Integrated High Performance Turbine Engine Technology (IHPTET) and High

Cycle Fatigue (HCF) programs and the NASA High Speed Civil Transport (HSCT) and Advanced Subsonic Technology (AST) programs.

### REFERENCES

1. "Aerodynamic Pressure and Temperature Measurement Through Fluorescence Lifetime Imaging," K. D. Grinstead, L. P. Goss, D. D. Trump, and J. R. Gord, Presented at the 39th Rocky Mountain Conference on Analytical Chemistry, 3-7 August 1997, Denver, CO.
2. "Recent Progress in PSP," A. E. Baron and G. Dale, Proceedings of the 5<sup>th</sup> Pressure Sensitive Paint Workshop, Arnold Lakeside Club, Tullahoma, Tennessee, May 14-16, 1997.
3. Private Communication with Mr. Tom Bahan (see Kodak ES-1.0 camera).
4. "Pressure Sensitive Paint Measurements Using a Phosphorescence Lifetime Method," A. G. Davies, Proceedings of the 7<sup>th</sup> International Symposium on Flow Visualization, Seattle, Washington, Sep. 1995.
5. "A Scanning Laser System for Temperature and Pressure Sensitive Paint," M. Hammer, B. Campbell, T. Liu, and J. Sullivan, AIAA Paper No. 94-0728.
6. "Fluorescent Lifetime Imaging," J. R. Lakowicz, et al., Analytical Biochemistry **1992**, *202*, 316.

## **APPENDIX A**

# **Pressure Sensitive Paint for Low Speed Applications Comparison of 1D-Scanning and 2D-Imaging Techniques**

Prepared by

School of Aeronautics and Astronautics  
Purdue University  
1282 Grissom Hall  
West Lafayette, IN 47907-1282

Submitted to

Innovative Scientific Solutions, Inc.  
2786 Indian Ripple Road  
Dayton, OH 45440-3638

### **PRINCIPAL INVESTIGATOR:**

John Sullivan, Professor and Head  
School of Aeronautics and Astronautics  
(765)494-5117  
e-mail – [sullivan@ecn.purdue.edu](mailto:sullivan@ecn.purdue.edu)



## Pressure Sensitive Paint for Low Speed Applications

Pressure Sensitive Paints (PSP) and Temperature Sensitive Paints (TSP) are being developed at numerous laboratory facilities around the world for both wind tunnel and flight measurements. (Refs. 1-3). The challenges in applying PSP to low speed flows are the inherent low pressure sensitivity ( 1% change in intensity for a 1 psi pressure change) and the temperature sensitivity of the PSP. These effects are illustrated by the calibration shown in Figure 1 for Ru(dpp) in RTV. The capabilities and challenges of using PSP in low speed flows were explored in two experiments: a normal impinging jet and an inclined impinging jet.

A low speed normal impinging jet test was used to demonstrate the increase in signal-to-noise ratio of the laser scanning system combined with optical chopping and lock-in amplification. These experiments determined the ultimate pressure resolution and accuracy available with this system because of the tightly controlled test conditions. The experimental setup used is shown in Figure 2. Pressure sensitive paint (Ru(ph<sub>2</sub>-phen) in GE RTV 118) is coated on the impinging surface and a 5 mm diameter nozzle is placed 10 mm from the plate. The paint is excited by an argon ion laser ( 457 and 488 lines), with an optical chopper modulating the beam. The scanning mirror scans a 0.2 mm laser spot across the plate. The luminescence is detected using a low noise photomultiplier tube with a 600 nm high-pass filter to only pass the fluorescence. The PM signal is connected to a lock-in amplifier which is then sampled with a PC.

Figure 3a shows the raw intensity distributions of the paint over a range of jet total pressures from 0.05 to 0.4 psid. The dip in the middle is from the jet partially blocking the fluorescence. The ratio of the signals ( $I_{ref}/I$ ) is shown in Figure 3b. Note that ratioing removes the effects of the uneven fluorescence signal from Figure 3a. The deviation of the intensity ratio from unity at large x/d indicates temperature effects at different total pressures.. Based on in-situ calibration, the pressure distributions can be obtained and are shown in Figure. 3c. This illustrates that the ruthenium based paint is capable of measuring pressures below 0.05 psi resolution better than 0.01 psi.

The second experiment was a joint effort between Purdue and ISSI to compare the Laser Scanning System and the CCD Camera System. The experimental set-up shown in Figure 4 utilizes a high speed ( near sonic) jet impinging on a flat plate at a shallow angle. This generates a low pressure distribution on the plate (shown at the top of Figure 4.) and a temperature distribution caused by heat transfer to the cold expanded jet.

Seven different paint formulations were tested.

Purdue Paints	Ru(dpp) in RTV
	PtTFPP in polystyrene
	Ru(dpp) on TLC Plate (silica gel)
	PtTFPP on TLC Plate
ISSI Paints	PtTFPP in toluene sol-gel a (ja089a)
	PtTFPP in ethanol sol-gel b (ja089b)
	PtTFPP in ethanol sol-gel c (ja089c)

Calibration curves obtained in the ISSI calibration chamber for the seven paints are shown in Figure 5 along with the Stern-Volmer constants.

Results for the tests shown in Figure 6 for the CCD Camera System and in Figure 7 for the Laser Scanning System demonstrate the complex nature of the inclined jet flowfield. For this case the jet stagnation pressure was  $P_o=27$  psia, giving a near sonic jet exit Mach Number. The expansion to this condition cools the jet, but entrainment of ambient air prior to and during impingement, generates a very complex heat transfer distribution. The image of the pressure and the laser scans on the plate should have only one peak, but the data shows two. Heat transfer has changed the surface temperature and the temperature sensitivity of the PSP causes the data to contain both temperature and pressure effects. In fact at the position of peak pressure (indicated on Figure 7) the intensity ratio should be greater than one but because of the temperature sensitivity it is actually less than one.

A common way to correct for a uniform temperature distribution is to use known pressures (an in situ calibration) to correct the data. Figure 8 shows the data reduced using an in situ and coupon calibration. Since the inclined jet causes a heat transfer with large spatial variations on the flat surface, a simple in situ calibration at one surface point is ineffective.

Laser scanning system results for the Ru(dpp) in RTV paint are shown in Figure 8 (intensity based) and Figure 9 (phased based). This paint is much less temperature sensitive than the PtTFPP on TLC, so results are closer to the expected pressure distribution but are still too corrupted by the surface temperature to give usable results.

An in situ calibration of the PtTFPP on TLC paint was performed using both the laser scanning and CCD camera systems. Results for the laser scanning system at the maximum pressure point are shown in Figure 11 and jet centerline scans from the CCD camera are shown in Figure 12. Note the order in which the data was taken. The highest pressure point was taken first (point 1) then the lowest pressure (point 2) followed by a set of points at increasing pressure. Not only should the data points have an intensity ratio greater than one, they should change monotonically with pressure. As in the previous data the temperature sensitivity of the PSP is playing a significant role but in addition the experiment was not in thermal equilibrium at each data point.

The following conclusions can be drawn from the two experiments:

1. When the thermal environment and boundary conditions are tightly controlled, as in the normal impinging jet experiment, PSP can give pressure measurements with a resolution of .01 psia.
2. The inclined jet experiment generated low surface pressures and high surface heat transfer with subsequent spatial and temporal surface temperature variations. Current PSP's are unable to separate the pressure and temperature effects under these extreme conditions. This experiment vividly points out the necessity of controlling and/or measuring the thermal environment and thermal boundary conditions when applying PSP's to low speed flows.

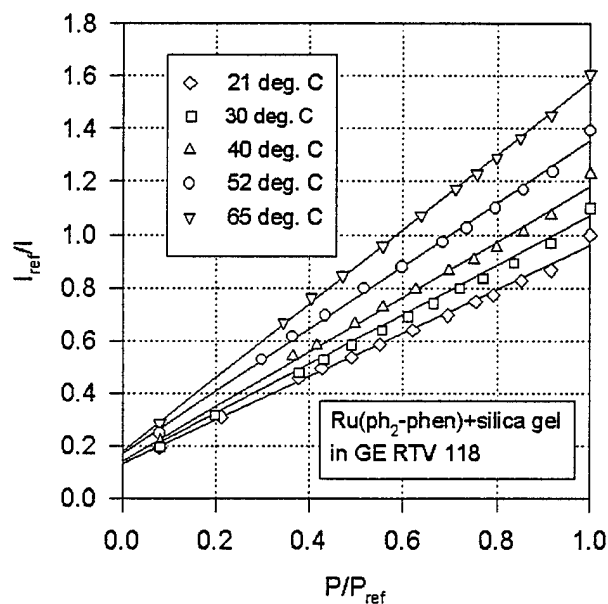


Figure 1. Calibration Curve

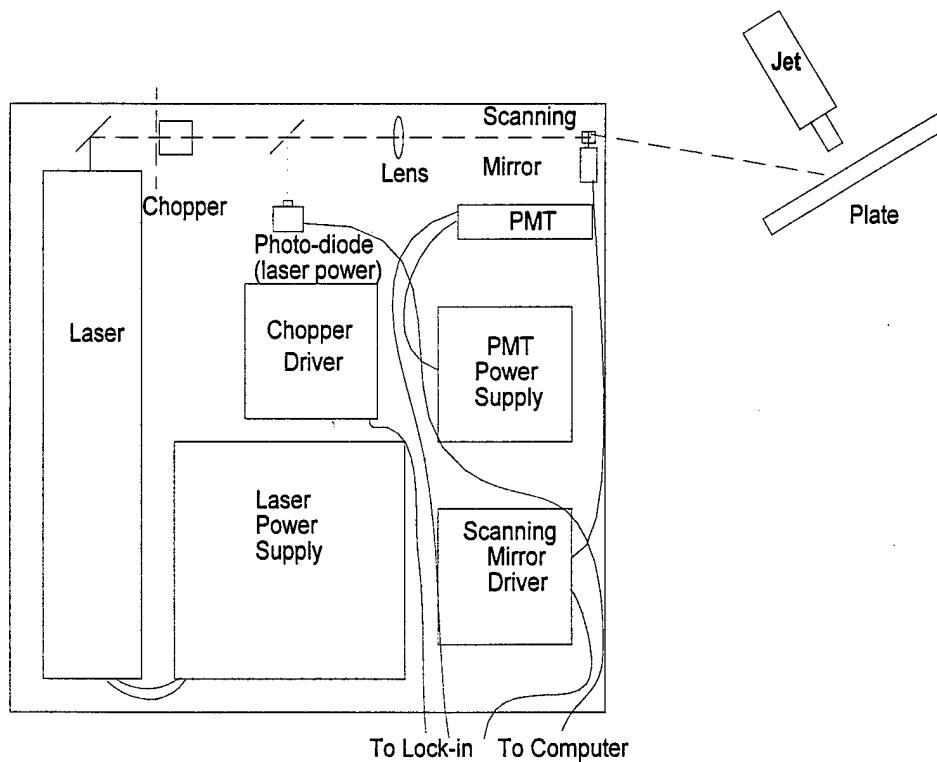


Figure 2. Normal Impinging Jet /Laser Scanning System Set-up

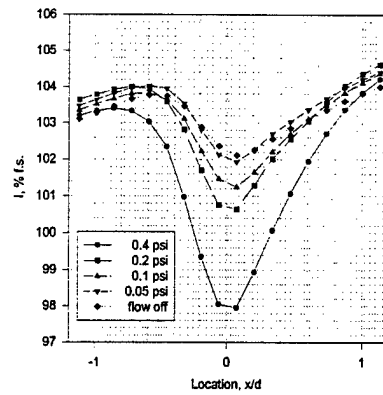


Figure 3a. Raw Intensity Signal – Normal Impinging Jet

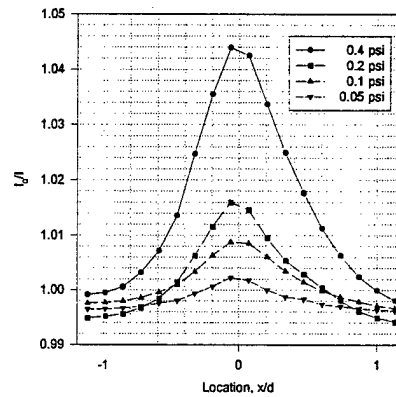


Figure 3b. Intensity Ratio-Normal Impinging Jet

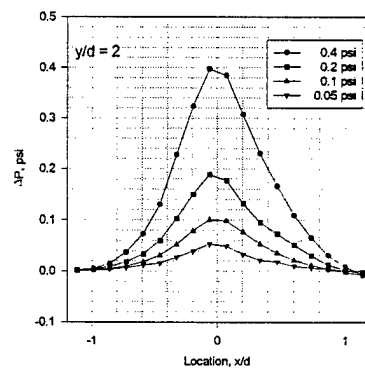
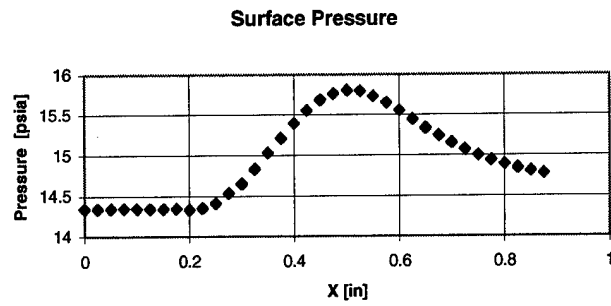


Figure 3c. Pressure Distribution – Normal Impinging Jet.



$P_o = 27$  psia

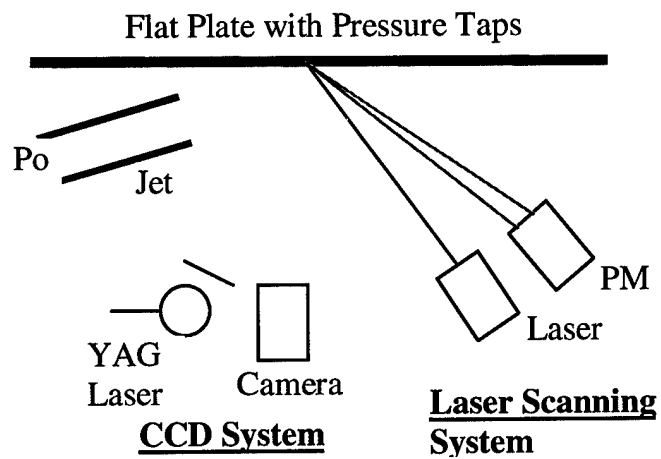


Figure 4. Purdue/ISSI Inclined Jet Set-up

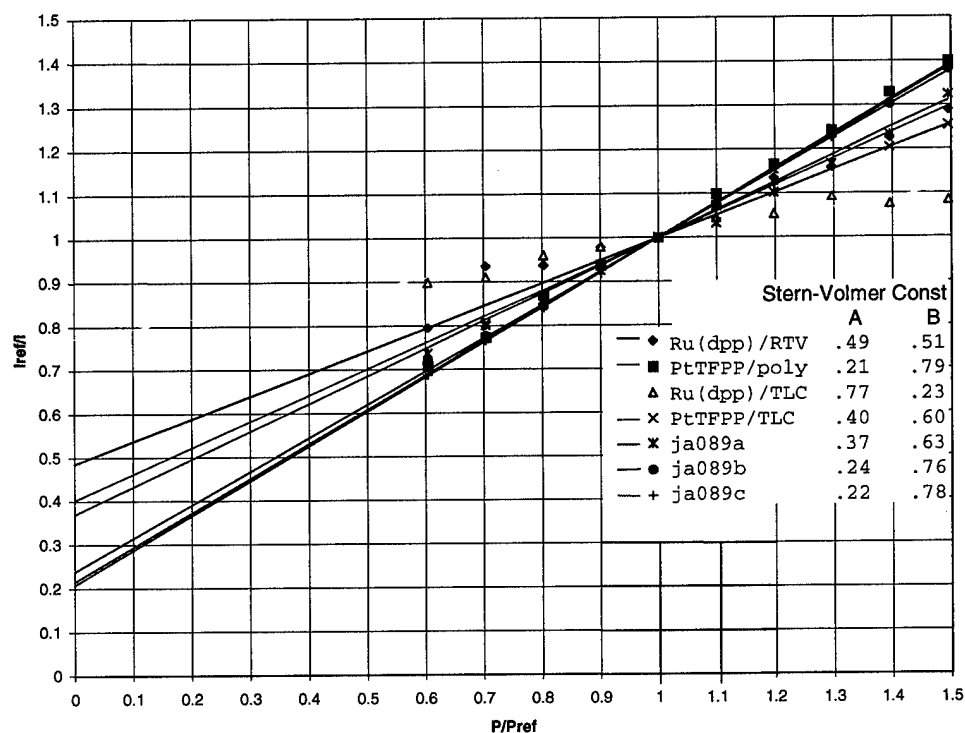


Figure 5. Coupon Calibration of the Seven PSP's Evaluated in the Purdue/ISSI Tests

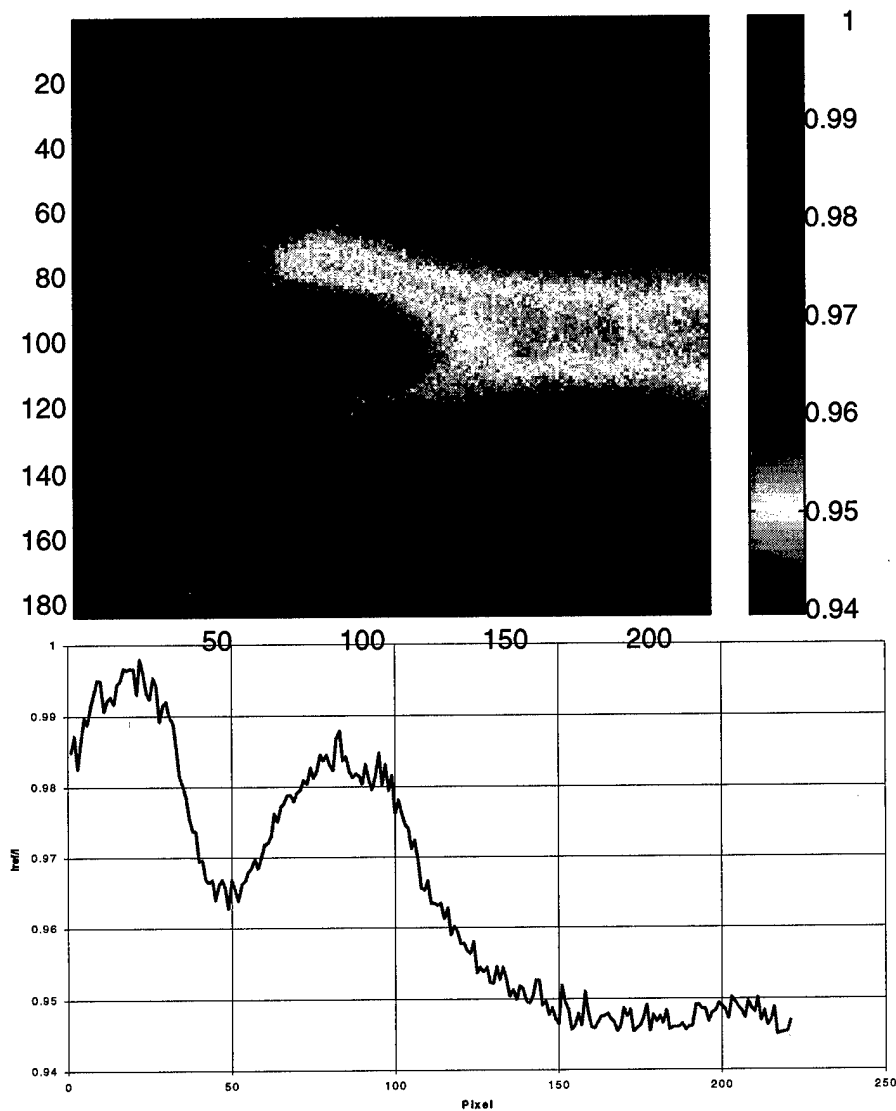


Figure 6. CCD Camera System Intensity Ratio – PtTFPP on TLC.

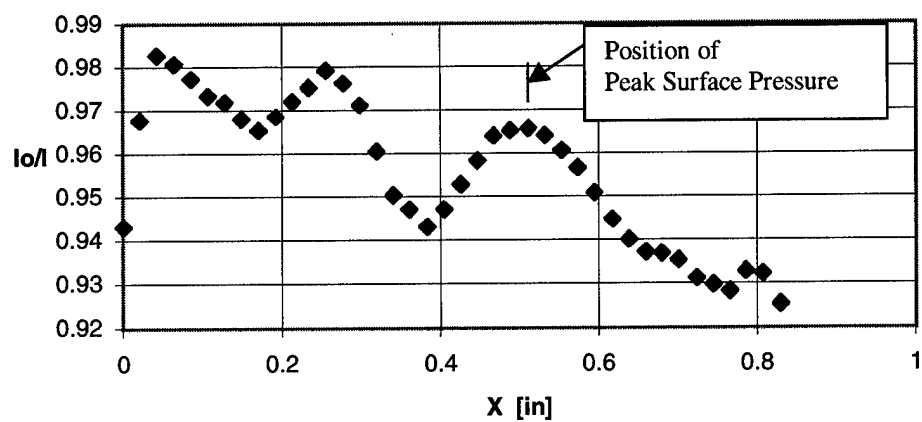


Figure 7. Laser Scanning System Intensity Ratio - PtTFPP on TLC

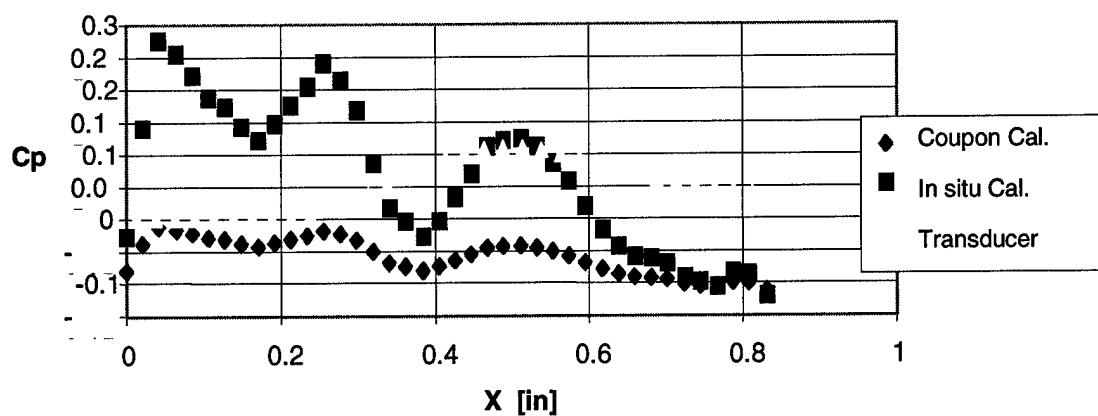


Figure 8. Comparison of Different Data Reduction Methods for the Inclined Jet -PtTFPP on TLC Laser Scanning System

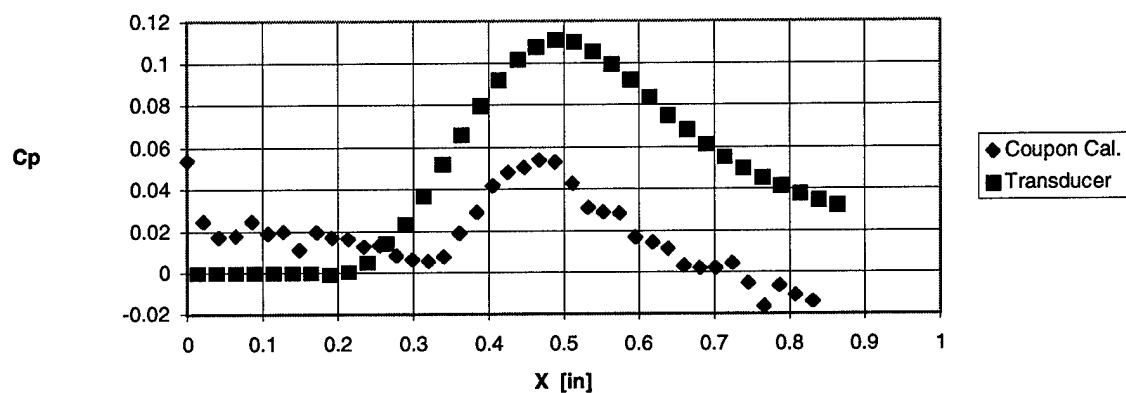


Figure 9. Comparison Data for the Inclined Jet -Ru(dpp) in RTV Laser Scanning System



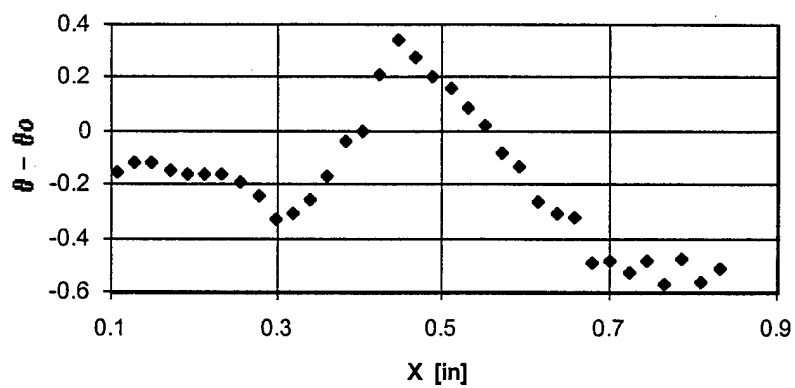


Figure 10. Phase Difference – Ru(dpp) in RTV – Laser Scanning System,

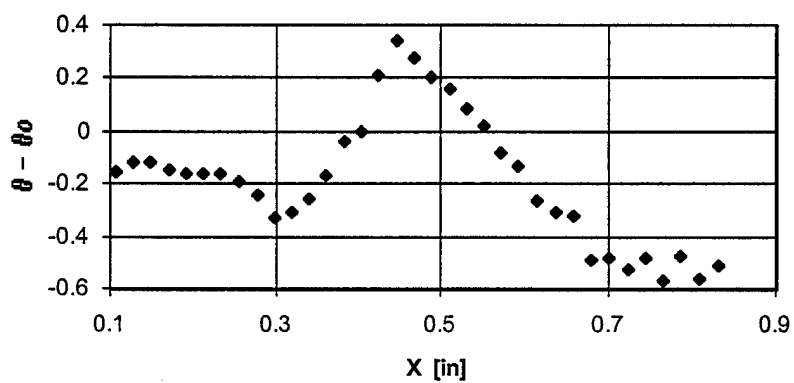


Figure 11. Laser Scanning In Situ Calibration – PtTFPP on TLC.

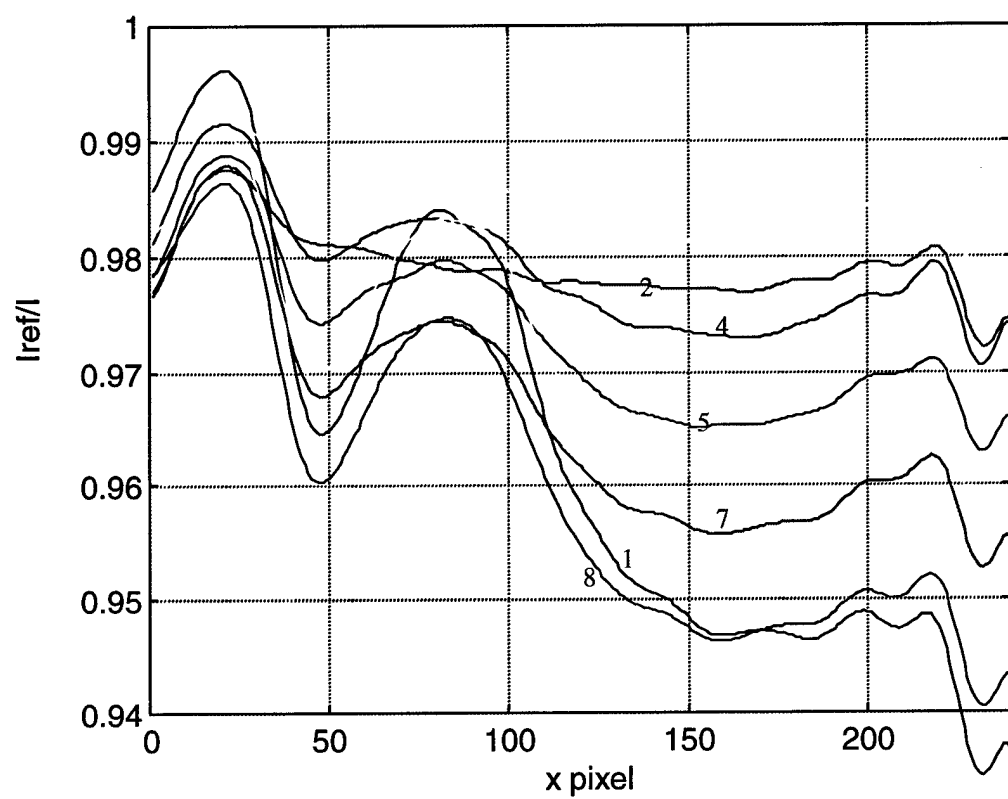


Figure 12 . CCD Camera System In Situ Calibration - PtTFPP on TLC

## Appendix

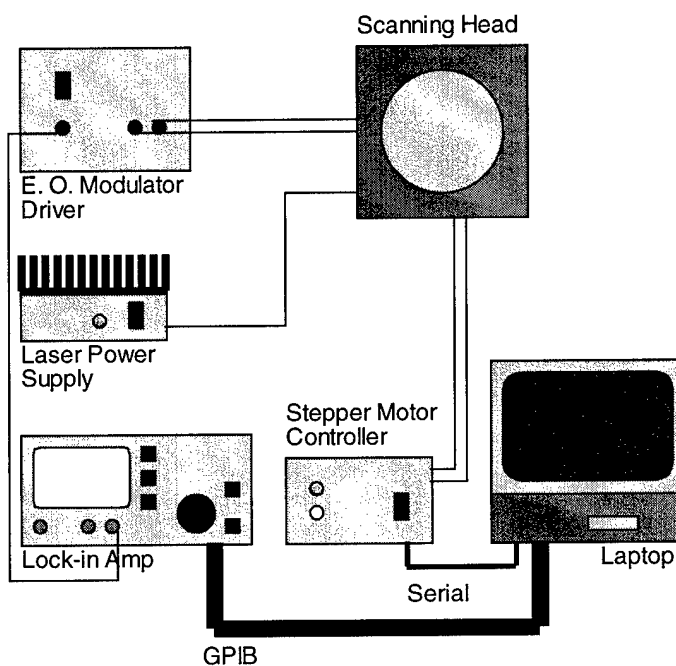
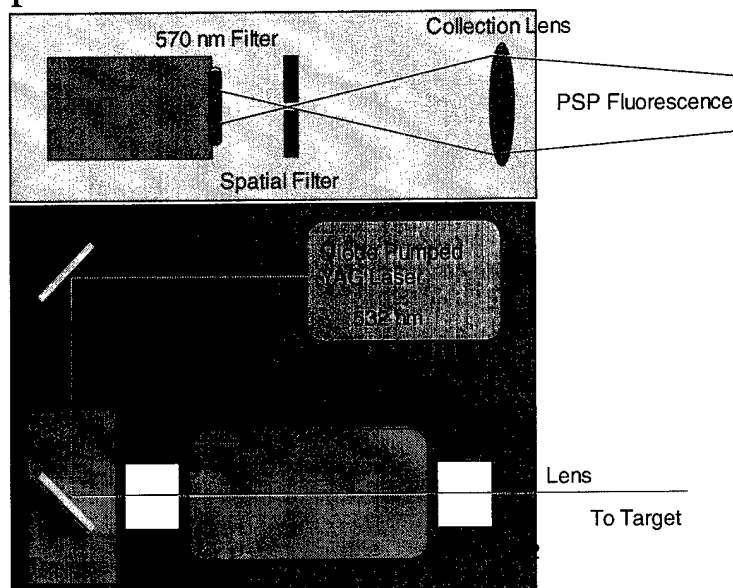
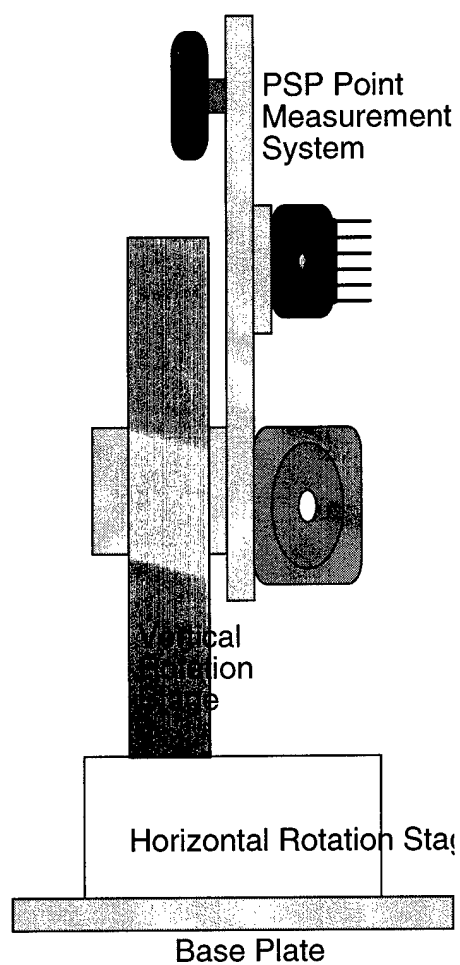


Figure A1. Diagrams of Laser Scanning System

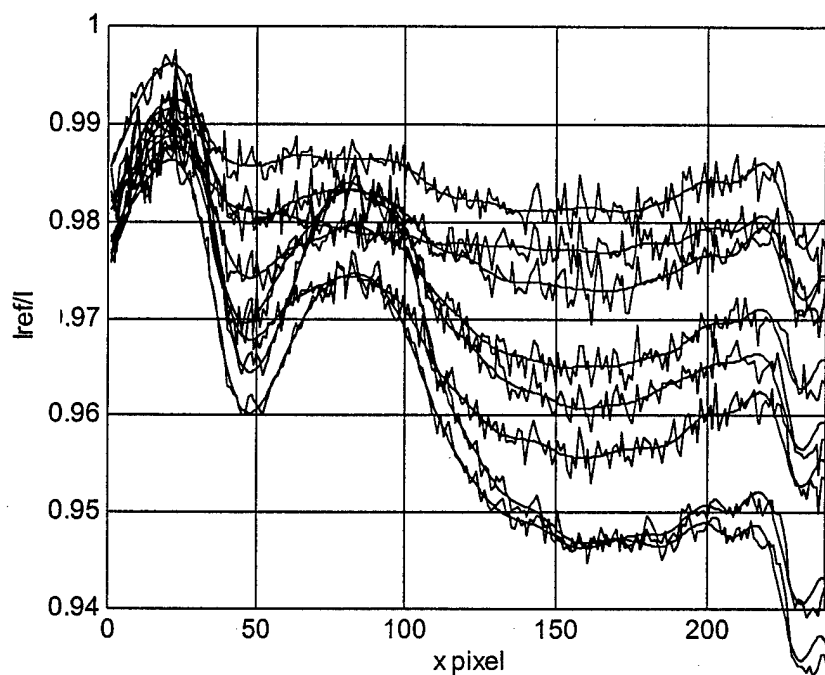


Figure A2. Comparison of CCD Camera Data – Filtered and Unfiltered – x direction  
PtTFPP on TLC

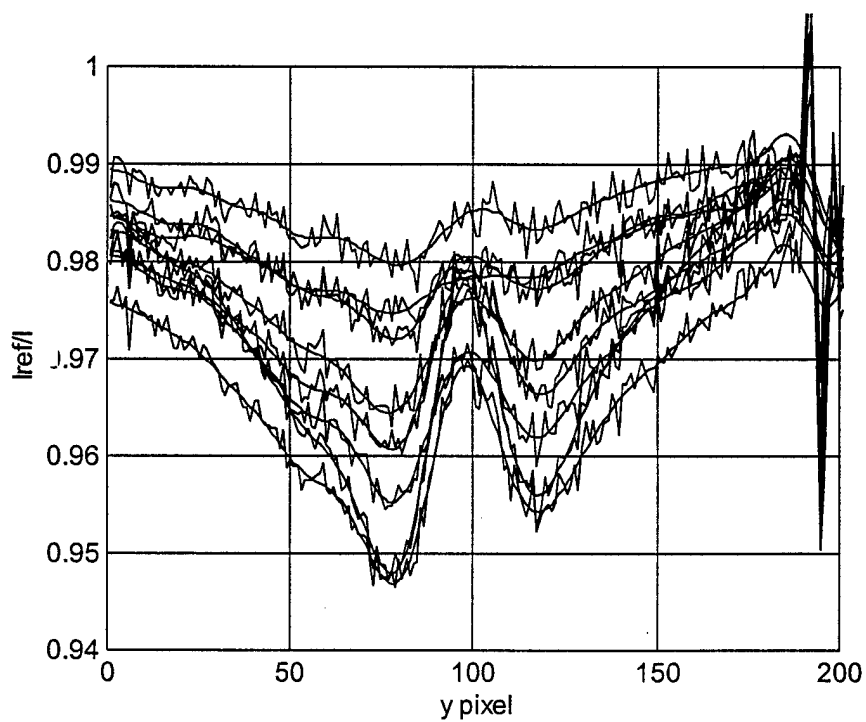


Figure A3. Comparison of CCD Camera Data – Filtered and Unfiltered – y-direction  
PtTFPP on TLC.

**APPENDIX B**

**MIT FINAL REPORT FOR STTR PROGRAM**

Prepared by

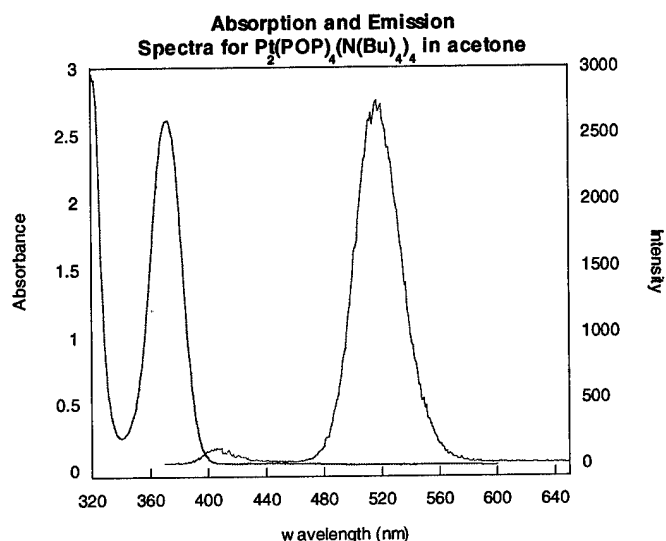
Professor Daniel Nocera  
Department of Chemistry  
Massachusetts Institute of Technology  
Cambridge Massachusetts

## MIT Research Final Report for STTR (PI Nocera)

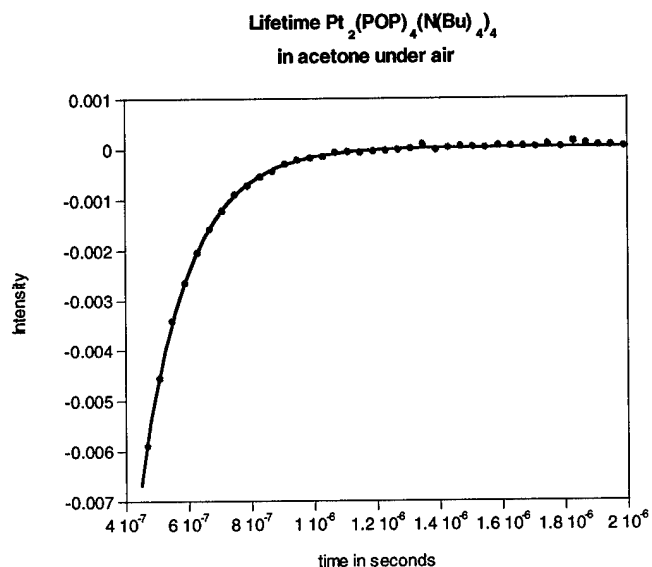
With our ability to control energy flow in molecules, we are poised to develop PSPs for the next generation of pressure measurements for the Air Force. Many of the problems confronted by porphyrin-based PSPs are overcome when the porphyrin is replaced by inorganic lumophores. Inorganic complexes are characterized by low energy vibrations, which are typically already populated at room temperature. Thus, if an inorganic complex is a bright emitter at room temperature, its luminescence will be maintained as the temperature is raised without the population of new thermally activated nonradiative decay channels. In this instance, the nonradiative decay rate (and hence intensity) will vary monotonically and slowly through a 20 to 100 °C temperature range. In addition, metal complexes are robust in the highly oxidizing environment of singlet oxygen. Finally, the lifetimes of inorganic lumophores may be systematically varied over a wide range allowing specific pressure ranges for measurement to be targeted. Two classes of compounds are primarily targeted,  $d^8-d^8$  and  $d^{10}-d^{10}$  metal dimers and polypyridyl complexes of  $d^6$  (e.g.,  $Ru^{2+}$  and  $Os^{2+}$ ) metals.

### *All-inorganic metal dimers for PSP applications*

We have surveyed the platinum dimer,  $Pt_2(pop)_4^{4-}$  ( $pop = \text{pyrophosphito}, \mu-P_2O_5H_2^{2-}$ ) during the first phase of the STTR. The platinum pop dimer was synthesized using phosphorous acid and  $K_2PtCl_4$  according to published methods[1]. This water-soluble compound is a tetra-anionic salt with potassium serving as the counter ion. The potassium salt is not conducive for our purposes as it is insoluble in most organic solvents, and decomposes slowly over the course of several hours in solution. To improve the solubility of  $Pt_2(pop)_4^{4-}$  in the solvents used in the synthesis of PSPs the compound is run down an ion exchange column to exchange the potassium cations for tetrabutylammonium cations  $[Bu_4N]^+$ . This affords excellent solubility in organic solvents such as acetone, alcohols, acetonitrile, and THF. Furthermore the stability of the tetrabutylammonium salt is significantly increased from hours in solution to days. The  $Pt_2(pop)_4^{4-}$  absorbs in the UV ( $\lambda_{max}=373 \text{ nm}$ ), and emits strongly in the visible ( $\lambda_{max}=518 \text{ nm}$ ). The absorption and emission spectra are overlaid below.



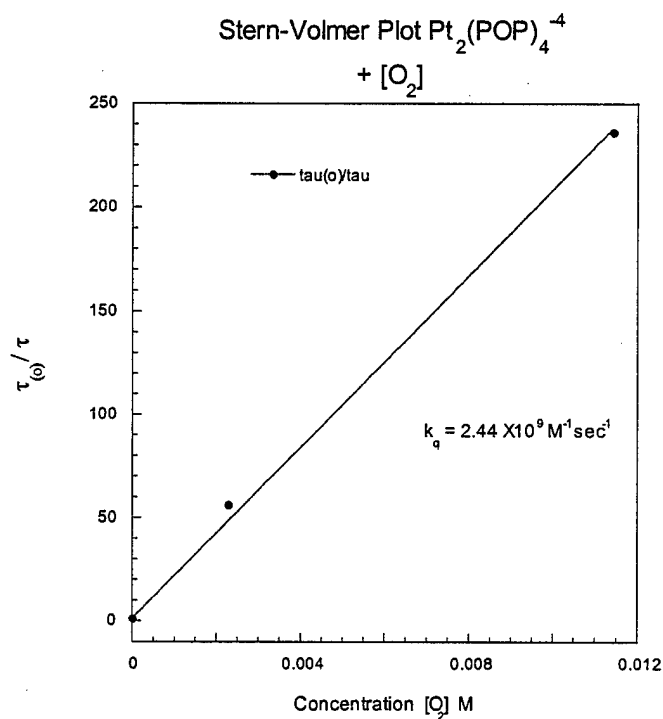
The tetrakis(diphosphito)diplatin(II) emits strongly in fluid solutions at ambient temperatures. The lifetime and quantum yield of  $\text{Pt}_2(\text{pop})_4^{4-}$  are both effected by the presence of quenchers. The lifetime of the platinum dimer dramatically changes as a function of the concentration of  $\text{O}_2$  present in the system. The lifetime under atmospheric conditions is 153 ns versus 8.4  $\mu\text{s}$  under ultra high vacuum. A typical lifetime is shown below.



A linear correlation exists between the concentration of the quencher and the relative observed lifetime of the excited state and which can be expressed as

$$\frac{I_0}{I} = \frac{\tau_0}{\tau} = 1 + k_q \tau_0 [O_2]$$

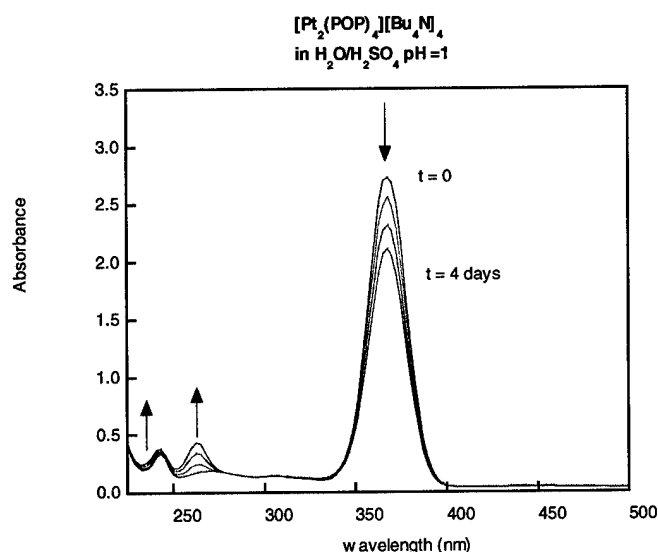
where  $I_0$  and  $\tau_0$  are the intensity and lifetime respectively when no quencher is present,  $I$  and  $\tau$  are the intensity and lifetime at a given quencher concentration, and  $k_q$  is the quenching rate constant. The ratio of  $\tau_0/\tau$  versus the  $O_2$  concentration in a Stern Volmer plot affords the quenching rate constant  $k_q$  from the slope of the line. In our case  $k_q$  is equal to  $2.44 \times 10^9$  (Msec)<sup>-1</sup>. A linear relationship is observed over the entire range of  $O_2$  concentrations at room temperature.



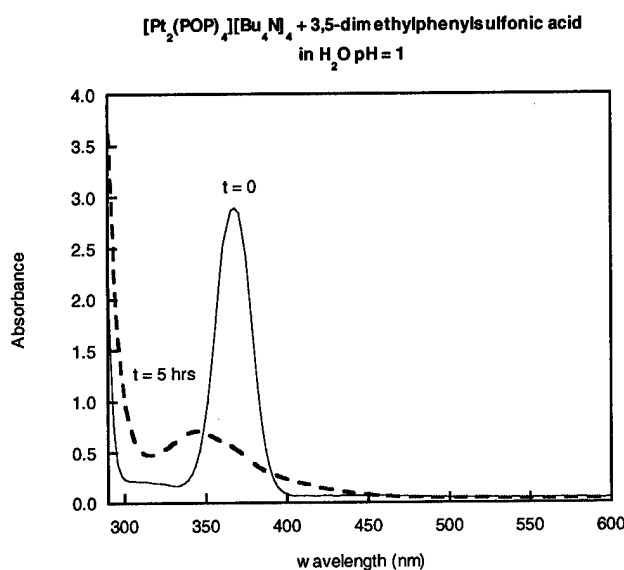
The excited state, of  $^3A_{2u}$  parentage ( $d\sigma^*p\sigma$  electron configuration), strongly luminesces in the 511-517 nm region with the quantum yield of 0.52 approaching that of laser dyes [2]. The phosphorescence, generated by exciting the large absorption cross-section of the molecule with a third harmonic of a Nd:YAG laser ( $\epsilon = 20,000 \text{ M}^{-1} \text{ cm}^{-1}$  at 353 nm), is readily quenched by oxygen. The lifetime of the excited state is 8.4  $\mu\text{s}$  and thus is ideal for low speed, high-pressure applications.



RTV silicone polymers of this complex have been prepared from acetone/toluene mixtures. As predicted from lifetime, emission quantum yield, and oxygen quenching rate constant measurements, PSPs based on this all-inorganic complex exhibit temperature sensitivities that are superior to that of Pt(II) porphyrins, presaging their implementation for high pressure PSP applications. However, we have observed that  $\text{Pt}_2(\text{pop})_4^{4-}$  paints exhibit degradation over time thereby limiting their utility. Photochemical studies have shown that the  $\text{Pt}_2(\text{pop})_4^{4-}$  excited state is capable of undergoing H atom abstraction reactions with the methyl group of toluene, which is a notoriously susceptible bond to activation. The possibility of this type of photoinduced decomposition pathway was investigated. It is known that in the excited triplet state  $\text{Pt}_2(\text{pop})_4^{4-}$ , can be quenched, by halogen atom transfer reagents (such as alkyl and aryl halides), as well as hydrogen donors such as isopropyl alcohol, tributyltin hydride and phosphorous acid. Since some of the preparations are carried out in the presence of toluene and alcohols a possible explanation for the lack of robustness found in this system is a consequence of the reaction conditions involved in the sample preparation. Stability tests were performed under varying conditions of pH, and presence of hydrogen atom donors.  $\text{Pt}_2(\text{pop})_4^{4-}$  was dissolved in water and this solution was then acidified with two different acids sulfuric and 3,5-dimethylphenyl-sulfonic acid. The dimer in neutral water shows significant decomposition in as much as just 10 hours by UV-Vis spectroscopy. The acidified solution (pH = 1) using sulfuric acid shows little change over a 24 hour period.



However at the same pH, a solution acidified with 3,5-dimethylphenylsulfonic acid was completely decomposed in just over 5 hours under the same conditions.

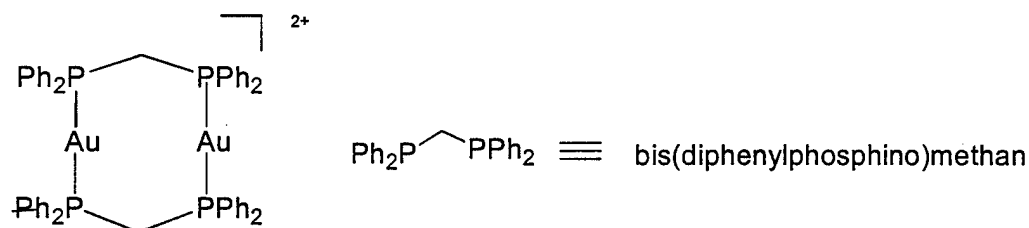


$\text{Pt}_2(\text{pop})_4^{4-}$  favors acidic conditions, and is susceptible to radical atom abstractions, from groups such as alcohols, halogenated aryls, and methyl substituted phenyl derivatives. These compounds should be avoided in the synthesis of PSPs including  $\text{Pt}_2(\text{pop})_4^{4-}$  to increase the stability of the active species.

Accordingly, the RTV solvent system will be modified to eliminate toluene as a solvent. We expect that this minor modification in procedure will afford stable RTV films. The lifetime, emission quantum yield and oxygen quenching rate constant of the all-inorganic PSP paint prepared by these modified procedures will be quantified and the paint will be calibrated for pressure measurements.

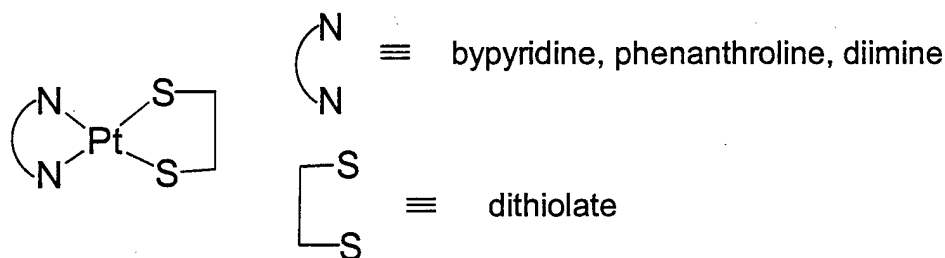
The desirable  $d\sigma^*p\sigma$  electron configuration is not restricted to  $d^8-d^8$  complexes. The  $d^{10}-d^{10}$  dimeric gold complexes of bidentate phosphines such as  $\text{Au}_2(\text{dppm})_2^{2+}$  also possess  $d\sigma^*p\sigma$  excited states that are intensely luminescent and of the appropriate  $\mu\text{s}$  lifetime for the desired PSP measurements ( $\phi_e = 0.31$ ,  $\lambda_{\text{max}} = 593 \text{ nm}$ ,  $\tau_0 = 21 \mu\text{s}$ ) [3]. Similar to  $\text{Pt}_2(\text{pop})_4^{4-}$  complexes, this excited state is susceptible to oxygen quenching [4]. The preparation of the

hexafluorophosphate salt of these complexes will permit the complexes to be dissolved in oxygen permeable matrices.



The gold dimer was synthesized as the hexafluorophosphate salt by a standard literature procedure[5]. The  $d^{10}$ - $d^{10}$  binuclear  $\text{Au}_2(\text{dppm})_2^{2+}$  complex, like binuclear  $d^8$ - $d^8$  metal systems such as  $\text{Pt}_2(\text{pop})_4^{4+}$ , possesses rich photochemistry. The complex has strong absorbencies in the Uv region at 290 and 267 nm, and photoluminescence centered around 570 nm. The low-lying triplet excited state is long lived, approximately 20  $\mu\text{s}$ , in fluid solution at ambient temperatures. Exposure to air results in severe quenching of the excited state via an energy transfer pathway. The quenching rate constant derived from a Stern Volmer plot of this compound shows a  $k_q = 2.0 \times 10^9 \text{ M}^{-1} \text{ sec}^{-1}$ .

### Square Planar Platinum Complexes



Square planar platinum(II) complexes have also been prepared. The square planar complexes are among the earliest studied transition metal luminophores. Most of the focus has been on Pt(II) complexes such as  $\text{PtX}_4^{2-}$  ( $\text{X}=\text{Cl}, \text{CN}$ ),  $\text{Pt}(\text{N-N})_2^{2+}$  ( $\text{N-N}$  = bipyridine, phenanthroline, and diimine), and  $\text{Pt}(\text{N-N})\text{X}_2$ [6]. Recently, Eisenberg and coworkers have synthesized a set of platinum diimine dithiolates, some of which show emissive properties at room temperature in fluid solutions[7]. A series of such compounds have been synthesized. So far [4,7-diphenyl-1, 10-phenanthroline][ethyl-2-cyano-3, 3'-dithiolatoacrylate]platinum(II) shows

the most promise with a long lived, 26  $\mu$ s, excited state and relatively high quantum yields when compared to other compounds in this class. However, Gray and Connick have recently shown that some analogous complexes under go photochemical oxidation to form sulfinates when irradiated in the presence of  $O_2$ [8]. Further study of this oxidation is warranted before these species maybe deemed suitable for PSPs.

### *Polypyridyl $d^6$ metal complexes*

PSPs based on the luminescence of polypyridyl complexes of  $d^6$  metal complexes have shown great promise in recent years. In light of the fact that the best results seen to date for our PSP systems are found for the tris(4,7-diphenyl-1,10-phenanthroline)Ru(II) complex, we are currently focusing on the synthesis of substituted ruthenium bipyridyl complexes. The work in this area has been prolific and the photophysics of these compounds are extremely well understood. For this reason we have been targeting ruthenium diimine complexes with superior quantum yields and lifetimes to study. These properties can be tailored to a great extent by altering the energy of the metal to ligand charge transfer excited state by systematically changing the substituents on the ligands.

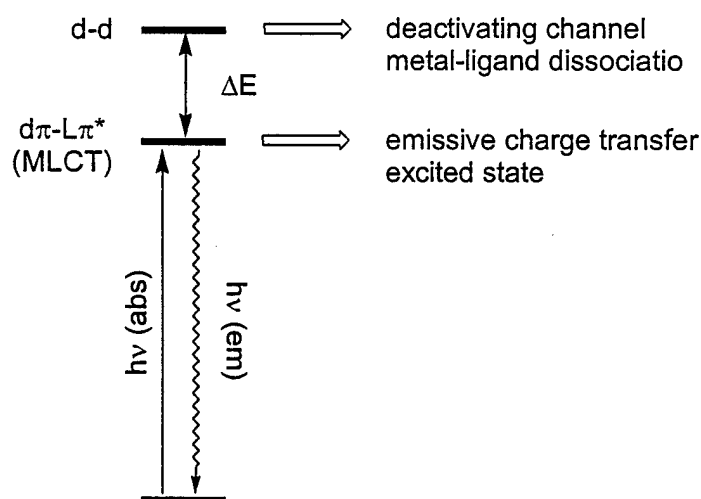


*Figure 1. Excited state structure of metal polypyridyl complexes to be implemented in the design of new PSPs for low speed, high pressure measurements.*

The pertinent excited state structure for these complexes is shown in Figure 1. A d-d ligand field state is energetically proximate to a lowest energy  $d\pi$  to  $\pi^*$  (polypyridyl) metal-to-ligand charge

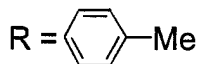
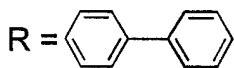
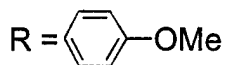
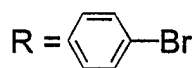
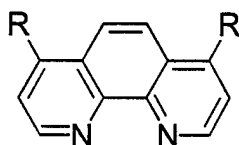
transfer (MLCT) excited state. The MLCT excited state is readily quenched by oxygen; hence it is the luminescence lifetime and intensity properties of this excited state that are at the underpinning of the PSP properties for this polypyridyl class of compounds. Because the ligand field state is metal-ligand antibonding, small energy gaps lead to efficient nonradiative decay (i.e., short lifetimes and small quantum yields) owing to deactivation along a ligand-metal dissociative reaction coordinate. The population of the deactivating state follows Boltzmann statistics (i.e.,  $\exp(-\Delta E/kT)$ ) with  $\Delta E = 1500\text{-}2500\text{ cm}^{-1}$  and thus these complexes can exhibit significant emission intensity dependencies over temperature ranges pertinent to oxygen pressure measurements. The key to minimizing the temperature sensitivity with regard to PSP applications is to design metal complexes with large energy gaps. Specifically, since the d-d ligand field energy is relatively constant for a given  $d^3$  or  $d^6$  metal, the MLCT excited state must be energetically stabilized relative to the d-d ligand field. This can be achieved by tuning the electronic properties of the polypyridyl ligand. Two carboxylate substituted bipyridine ruthenium compounds have been synthesized and isolated in good yields. Their sensitivity however proved to be inferior to the 4,7-diphenyl-1,10-phenanthroline derivative. This is not a surprising result when one considers the data in Table I. Relative to the Ru(II) tris bipyridyl (bpy) and tris phenanthroline (phen) benchmarks for this series of compounds, the dpphen complex exhibits one of the lowest energy MLCT excited states. Accordingly, the large energy gap engenders a luminescent excited state with appreciable luminescence intensity and an appropriate lifetime for PSP applications. The Ru(II) dpphen complex represents only the "tip of the iceberg" for high temperature PSP measurements. As Table I shows, there are other polypyridyl candidates that exhibit superior photophysical properties in comparison to the dpphen complex.

*Table I. Representative  $d^6$  Polypyridyl Complexes for the Design of New PSP Paints for Low Speed Pressure Measurements*

<i>Compound</i>	$\tau / \mu s$	$\phi_e$
$\text{Ru(bpy)}_3^{2+}$	0.89	0.062
$\text{Ru(phen)}_3^{2+}$	0.50	0.028

$\text{Ru}(\text{dpphen})_3^{2+}$	4.68	0.366
$\text{Ru}(4,7\text{-bpmo-phen})_3^{2+}$	5.95	0.237
$\text{Ru}(4,7\text{-bbr-phen})_3^{2+}$	5.93	0.403
$\text{Ru}(4,7\text{-bmo-phen})_3^{2+}$	6.1	0.387
$\text{Ru}(4,7\text{-bph}_2\text{-phen})_3^{2+}$	7.2	0.36
$\text{Ru}(4,7\text{-dtol-phen})_3^{2+}$	6.43	0.28
$\text{Os}(\text{phen})(\text{dppy})_3^{2+}$	3.6	0.36
$\text{Os}(\text{phen})(\text{diars})_3^{2+}$	4.3	0.44

The ligands we have targeted to synthesize and complex to Ru(II) are shown below



The synthetic starting materials for all these derivatives have been synthesized, and we expect to have all of these compounds in hand in the very near future.

In addition to the Ru(II) complexes listed in Table I, we are designing new PSP imaging based reagents. The energy of the MLCT can be precisely tuned with electron withdrawing and donating groups appended to the polypyridyl ligand. We designed a spectroscopic protocol for the measurement of the MLCT energies,

$$\Delta G_{\text{es}}^0 = E_0 + \chi$$

$$\chi = (\omega_{0,1/2})^2 (16k_B T \ln 2)^{-1}$$

where the excited state energy ( $\Delta G_{es}^0$ ) is related to the energy of the luminescence maximum ( $E_0$ ) and the reorganization energy ( $\chi$ ) containing solvent and low frequency modes, which are treated classically and related to the full width at half-maximum, ( $\omega_0, 1/2$ ). Thus from a simple measurement of the emission profile, the MLCT excited state, and consequently the crucial  $\Delta E$  parameter of Figure 1 may be determined.

We will expand studies to other metals including Os(II). Because, Os(II) metal-ligand bonds are generally stronger than its Ru(II) transition metal counterpart, the emission quantum yields and lifetimes are generally larger. Two representative compounds that we will prepare are listed in Table I; these complexes will be incorporated into sol-gel and RTV based paints during the next phase of the STTR.

## References

1. Sadler, P.J.; Pinto, F. D. R.; Filomena, M. A.; Subbiah, A.; Sanderson, M. R.; Neidle, S. J. *Chem. Soc. Chem. Comm.*, **1980**, 13.
2. Roundhill, D. M.; Gray, H. B.; Che, C.-M. *Acc. Chem. Res.* **1989**, 22, 55.
3. King, C.; Wang, J.-C.; Khan, N. I.; Fackler, J. P. *Inorg. Chem.* **1990**, 28, 2145.
4. Che, C.-M.; Kwong, H.-L.; Yam, V. W.-W.; Cho, K.-C. *J. Chem. Comm., Dalton Trans.* **1989**, 885.
5. Che, C.-M.; Kwong, H.-L.; Yam, V. W.-W.; Cho, K.-C. *J. Chem. Comm., Dalton Trans.* **1990**, 321
6. Fleischauer, P. D., Adamson, A. W., Sartori, G. *"Progress in Inorganic Chemistry"*, 17, Edwardsiley; New York, **1972**.
7. Zuleta, J. A., Mitch, S. B., and Eisenberg, R. *Coord. Chem Rev*, **97**, **1990**, 47.
8. Connick W. B., Gray H. B., *J. Am. Chem. Soc.*, **1997**, 119, 11620.